Geoheritage (2026) 18:5
https://doi.org/10.1007/s12371-025-01226-x

ORIGINAL ARTICLE

Geological, Cultural, and Archaeological Heritage Integrated into a Tourism Route Through the Main Granite Source Area Supplying Ávila's World Heritage Site

F. J. López-Moro[1] · M. López-Plaza[2] · J. I. García de los Ríos Cobo[3] · M. González Sánchez[1] · A. Herrero-Hernández[4]

Received: 19 June 2025 / Accepted: 12 November 2025

Abstract
This work presents a series of points of geological, cultural and archaelogical heritage that allow for the development of tourism routes in the most significant extractive area that supplied natural stone to the primary historical monuments of the city of Ávila, a World Heritage City. The conceptualization of this route is predicated on a multidisciplinary study encompassing an inventory of quarries, geological cartography, a documentary search, petrological, geochemical and structural work. The study identified five distinct granitic facies, all of which have been utilized in the construction of Avila's monuments, three of which have not been previously documented in cartographies. The petrological and geochemical investigation has facilitated the establishment of the sequence of emplacement of the distinct granitic facies, their classification, the explanation of compositional variations, their probable cogenetism, and the genesis of certain geological mesostructures. The structural study has revealed the existence of families of joints that controlled the size and shape of the dimension stone, which in turn has conditioned their use in the monument and the feasibility of exploitation. The inventory of the quarries has facilitated the analysis of the conventional techniques of cutting and the establishment of a size evolution of the wedge slots and the shape and size of quarries. The study's findings have been compiled into 13 points of interest. Visitors can gain a comprehensive understanding of the region's geology and its cultural and archaelogical heritage. This includes evidence of quarrying activities dating back to pre-Roman times.

Keywords Historical quarry · Tourism route · Granite · Ávila · Wedge slot · Cogenetic granite magmas

✉ F. J. López-Moro
fj.lopez@igme.es

M. López-Plaza
milplaz@usal.es

J. I. García de los Ríos Cobo
jigarciarioscobo@gmail.com

M. González Sánchez
maria.gonzalez@igme.es

A. Herrero-Hernández
antonio.herrero@unir.net

[1] Oficina de Salamanca, IGME-CSIC, Plaza de la Constitución 1, Salamanca 37001, Spain

[2] Dpto. Geología, Facultad de Ciencias, Universidad de Salamanca, Salamanca 37008, Spain

[3] Sociedad de Investigación y Explotación Minera de Castilla y León, S.A, Av. Rodrigo Zamorano, Boecillo, 47151 Valladolid, Spain

[4] Dpto. Educación, Facultad de Ciencias de la Educación y Humanidades, Universidad Internacional de La Rioja, 26006 Logroño, Spain

Introduction

Historical quarries, which have provided natural stone for the construction of monuments and emblematic buildings, are a fundamental resource for the conservation of architectural heritage. Their preservation is imperative not only to ensure the proper restoration of these monuments but also to preserve a cultural, geological, and landscape legacy that constitutes part of the identity of many cities. Nonetheless, a considerable number of historical quarries are at risk due to factors such as abandonment, uncontrolled exploitation, or urban sprawl. These factors impede the feasibility of restorations that are faithful to the original materials. In addition to their function as a source of materials, historical quarries possess a distinctive geological value. They act as a repository for the natural process that has formed these rocks over vast temporal periods. In a multitude of instances, these quarries play a pivotal role in facilitating research

Published online: 11 December 2025

endeavors. They offer a unique opportunity for scientists to thoroughly study the complex geological processes that underpin the formation of quarried rocks. Moreover, these quarries possess a cultural and historical dimension, having been exploited by generations of stonemasons who developed specific quarrying and carving techniques. In numerous locations, the tradition of quarrying has been transmitted as a trade from generation to generation (e.g., the stonemasons of Cardeñosa village, nearby Ávila), thereby becoming an integral component of the cultural heritage of the community. From a landscape perspective, historical quarries have significantly influenced the environment of historic cities. The loss of these features can disrupt the natural equilibrium, thereby altering the relationship between the built environment and its natural surroundings. The preservation of these quarries aligns with sustainability criteria, underscoring the importance of environmental stewardship. The judicious management of these sites prevents the disruption of pristine environments and the subsequent need for new quarries in undisturbed areas, thereby reducing ecological footprints. Furthermore, the integration of these quarries into educational or tourist infrastructure can serve to underscore their significance in the development of our built heritage. Similarly, the geological and landscape features of an area can be regarded as key elements of cultural and scientific interest, as well as instruments for promoting sustainable tourism—specifically, geotourism (Hose 1995; Dowling 2010). The interpretation of geological heritage can also be considered a central component of the geotourism experience, fostering public education (geoeducation) and enhancing the value of geotouristic assets (Hose 2000). Geological heritage encompasses not only scientific value but also cultural, aesthetic, and educational dimensions, which can be effectively conveyed through geotouristic initiatives (Reynard 2008).

The city of Ávila is one of 15 Spanish cities designated a World Heritage Site by the United Nations Educational, Social and Cultural Organization (UNESCO). It contains a historic monumental complex that includes the best-preserved wall in Spain, a cathedral-fortress, and a group of churches, convents, and palaces in which natural granite stone has been the almost exclusive building material (Fig. 1) (Moreno Blanco et al. 2022). The constructive history of the city and its environs is believed to have originated with the "Vettons" (Ayuntamiento de Ávila 2025), a Celtic people who primarily engaged in cattle husbandry and were renowned for their granite fortifications, known as "castros". In the Middle Ages, especially during the Romanesque period (12th and 13th centuries), the architectural materials used in the construction of Ávila were mostly altered silicified granites, exclusively from the vicinity of La Colilla (García-Talegón 1996). This was followed by a transition to fresh, coarse-grained granite rock during the Gothic era. The 16th-century witnessed a shift towards the use of medium and fine-grained granites, often containing nodules, in the construction of Renaissance palaces, as documented by Moreno Blanco et al. (2022)d pez-Plaza (2024). Historical documentation ascribes the provenance of these granitic materials to historical quarries in the environs of Ávila city, as well as in the municipalities of Cardeñosa, La Colilla, La Alameda and Palenciana (López Fernández 2002). Other nearby granitic areas, such as La Alamedilla del Berrocal, Mingorría, and El Calvario's Hill have also reported as extractive areas (López-Moro et al. 2021). However, the area of Cardeñosa is considered the most important supply center for the monuments of Ávila (Moreno Blanco et al. 2022; López-Plaza 2024) and the monuments north of Cardeñosa (Azofra Agustín and López-Plaza 2020).

However, the number of granitic facies found in Ávila's monuments (Moreno Blanco et al. 2022; López-Plaza 2024) is larger than those found in Cardeñosa's geological cartographies (Fig. 2B). This raises reasonable doubt about whether this area actually supplied so much material, or other causes explain this discrepancy. Additionally, no systematic studies have been conducted to quantify the number of old and recent quarries or to determine how much rock has been extracted over time. It is also unclear whether all the granitic types in this area were exploited and, if so, which ones were exploited the most and why. The Cardeñosa area, on the other hand, is exceptional. There, granite rock has been extracted from pre-Roman times until now, with significant changes in the tools used. This should leave

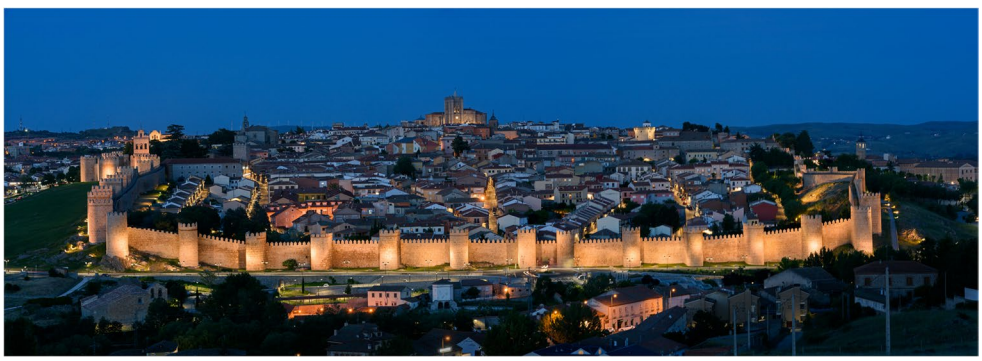

Fig. 1 Panoramic view of the old part of Ávila, a UNESCO World Heritage City. Photo courtesy of Ávila City Council

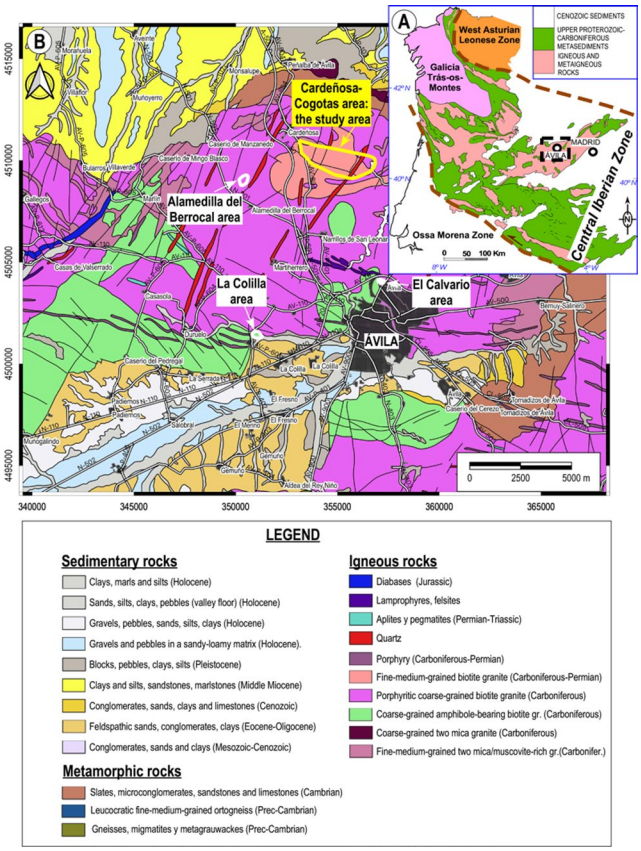

Fig. 2 (**A**) Geological map showing the different zones of the Iberian Massif and the location of the study area (dashed square). (**B**) Geological map of the surroundings of the World Heritage Site of Ávila with the quarry areas according to López-Moro et al. (2021) and the study area (yellow line). Topographic base in B according to ©Junta de Castilla y León and geologic base according to IGME (1982). Coordinate reference system: ETRS89/UTM Zone 30 N

a distinct mark on the stone cutting and the size of the quarry itself (García de los Ríos Cobo 2018). However, this has not been studied at this extraction center or many others. Therefore, the scientific community and the general public will welcome any findings concerning this issue. Sites where these findings can be displayed could become popular tourist and academic destinations. Furthermore, recent geological studies in the Cardeñosa-Cogotas area (López-Moro et al. 2021) revealed distinctive and unusual geological mesostructures with significant scientific and geotouristic value. In fact, many of these structures were must-see locations for geologists specializing in petrology, geochemistry, and mineralogy at the 11th Spanish Geological Congress in Ávila in 2024. Therefore, the Cardeñosa area merits recognition for its paramount significance as the preeminent provider of fresh granite to the city of Ávila. Moreover, this area exhibits distinctive features across the domains of geology, history, and quarrying, which collectively substantiate its immense potential for cultivating tourism routes. This study presents the main objective of designing a touristic itinerary with several selected points of interest (POI) in the Cardeñosa area. This will serve to protect the most remarkable elements of the geological, historical, and archaeological heritage, which would otherwise fall into oblivion and often succumb to destruction and decay. To achieve this primary objective, a substantial amount of geological, historical, and archaeological information must be generated. This information will also facilitate the attainment of secondary objectives including: (i) refining existing local geological cartographies; (ii) geologically and geochemically characterizing the exploited granitic facies; (iii) geochemically comparing monument and quarry rocks to determine provenance; (iv) establishing the geological processes that formed the area's characteristic geological mesostructures and the physical conditions under which they formed; (v) identifying structural elements in the granite that affect the exploitability of each facies and the size of the extractable blocks; (vi) creating an inventory of quarries in the area and differentiating ancient from modern; and (vii) establishing the evolution of techniques for cutting and exploiting granitic rock over time.

Study Area

The geographical area of this study encompasses the foothills of the municipality of Cardeñosa, including the Castro de las Cogotas (Figs. 2B and 3A). The rationale behind the selection of this particular area is articulated as follows. A thorough examination of the area revealed that this zone is home to nearly all the local quarries, encompassing both historical and contemporary excavations. These quarries exhibit a diverse array of cutting and extraction techniques, showcasing contrasting styles. The region is distinguished by the presence of geological phenomena, including balance rocks in the peneplain and network zones, piecemeal stopings, roof pendants, syn-plutonic dykes, miarolitic cavities, and chilled margins in exceptional outcrops in proximity to the Vetton hillfort of Las Cogotas, where a vertical section traversing several tens of meters unveils this array of geological structures. Moreover, the region boasts a plethora of archaeological and historical heritage sites, including the Vetton hillfort of Las Cogotas and numerous millstones dating from various periods, from the pre-Roman to the medieval eras. The presence of an archaeological classroom in Cardeñosa city further substantiates the organization of numerous excursions around the Vetton hillfort. This classroom serves as an ideal point of departure for the introduction of new routes related to ancient quarries and geology

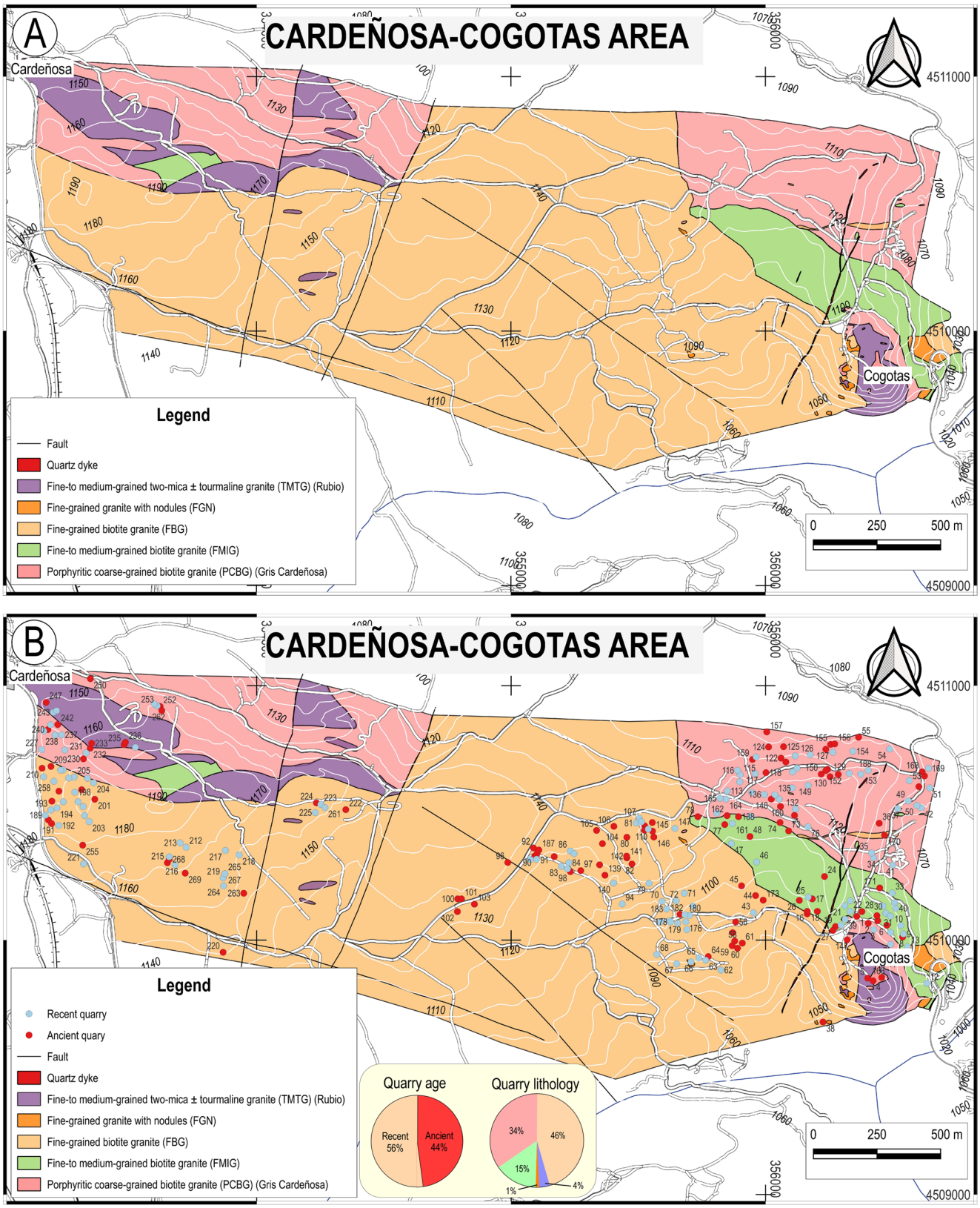

Fig. 3 (**A**) Detailed geological map of the Cardeñosa-Cogotas area. (**B**) Location of ancient and recent quarries in the Cardeñosa-Cogotas area. The proportions of the ancient and recent quarries and the lithologies of the quarries are included (circle plots). Topographic base according to ©Junta de Castilla y León. Coordinate reference system: ETRS89/UTM Zone 30 N

heritage. In summary, the area encompasses all requirements to achieve the main goal and secondary goals of this study.

Geological Setting

Ávila and its historical quarries are located within the Iberian (or Hesperian) Massif, which is composed of Ediacaran and Paleozoic materials, including abundant Variscan plutonic rocks. The Ediacaran rocks were deformed by the Cadomian orogeny, and especially by the Variscan orogeny. The Paleozoic rocks were mainly deformed during the Variscan orogeny. Both the Ediacaran and Paleozoic materials occupy much of the western half of the Iberian Peninsula and are bounded by Mesozoic and Cenozoic formations.

The Iberian Massif, in turn, is a segment of the European Variscan chain. This chain, in the Iberian Massif, has been divided into six zones: Cantabrian Zone, Asturoccidental-Leonese Zone, Galicia-Trás-os-Montes Zone, Central-Iberian Zone, Ossa-Morena Zone and South-Portuguese Zone (Vera et al. 2004) (Fig. 2A). Both the Cantabrian and the South-Portuguese zones seem to correspond to external chain zones, and the rest to internal zones, characterized by polyphase ductile deformation accompanied by regional metamorphism and synorogenic magmatic activity. Within this zonation, the study area is included in the so-called Central Iberian Zone (CIZ) (Fig. 2A), which is the most extensive of the Iberian Massif. Furthermore, this zone is the innermost domain of the chain and is characterized by extensive plutonism and wide variations in metamorphic grade. On a smaller scale, the study area could be assigned to the Western Domain of the Spanish Central System as defined by Bellido et al. (1981).

Four phases of Variscan deformation plus a fracturing phase have been distinguished in the area (IGME 1982). The first deformation phase (D1) is responsible for large, kilometer-scale folds that produce a flow schistosity (S1). The second deformation phase (D2) produces large folds and NE-vergent thrusting, an S2 schistosity, which is of strain-slip type in the chlorite zone and flow in the biotite zone. In addition, minor folds and lineations, both crenulation and intersection, are common. The third deformation phase (D3) produces subvertical axial plane folds, an S3 schistosity, which occurs only locally. The fourth deformation phase (D4) is considered late Variscan and produces kink-type folds. Finally, there is a fracture tectonics affecting Ediacaran, Paleozoic metasediments and granitic rocks, producing diaclases and E-W faults, infilled by lamprophyre, diabase and granitic porphyries. Later, there is another NE-SW system filled by quartz, forming the so-called "sierros".

The lithostratigraphy of the basement in the study area is composed of Ediacaran-Cambrian sedimentary series, with pelitic gneisses, migmatites, chloritic schists with intercalations of epidotites and limestones (IGME 1982). Below the gneisses and migmatites are glandular gneisses of Ordovician age (e.g., Talavera et al. 2013). The pelitic gneisses, migmatites and gneisses of the Ollo de Sapo Formation have been affected by a polyphase regional metamorphism of high grade and low Variscan pressure, which has reached the sillimanite-potassium feldspar zone. This metamorphism is followed by another, defined by remains of opaque and fibrolite within andalusite phenoblasts, and by dystene in aligned crystals in the process of transformation to andalusite. This metamorphism would be of at least intermediate pressures.

According to IGME (1982), two types of granitoids separated in time can be distinguished in the area. The first consists of Carboniferous two-mica granites emplaced in relation to the D2 Variscan folding (IGME 1982). They mainly occupy a NW-ESE trending belt that extends from Peñalba de Ávila to the vicinity of Mingorría (Fig. 2B). The second one is post D3 granitoids, including Carboniferous coarse-grained, sometimes porphyritic, biotite granites and amphibole-bearing granodiorites, together with Carboniferous-Permian fine-to-medium-grained biotite granites (Fig. 2B). Finally, there are post-Variscan subvolcanic igneous rocks (granitic porphyries, lamprophyres and diabases) emplaced at different stages in relation to the fracturing of the granites.

As for the cover materials in the area, they are all sediments ranging from the end of the Mesozoic (Upper Cretaceous) to the Holocene, with Neogene Cenozoic materials being by far the most abundant. They consist of lateritic soils, conglomerates, sandstones, clays, and calcareous materials (Fig. 2).

Methodology

A comprehensive approach was adopted to ensure the acquisition of exhaustive geological data. This approach entailed the following methodologies: (1) geological mapping, (2) mesoscopical study of granite types, (3) petrographical analysis, (4) geochemical study, (5) intensive variable constraints study, (6) comprehensive inventory of quarries, and (7) blocometry study. Besides, a meticulous examination of rock cutting and extraction methodologies was addressed. Furthermore, samples of the main granite facies found in Ávila monuments were taken from the Mosén Rubí church (Ávila) to determine if there are different geochemical patterns between the monument's rock and that of its quarry. These methodologies were executed with the objective of

generating the most comprehensive geological information possible to facilitate the development of touristic routes through the extraction centers.

The geological mapping phase led to the discovery of highly unusual mesostructures within granitic petrology (especially around the Cogotas hillfort), which were mapped, located, and thoroughly studied based on published scientific documentation. The quarry inventory was carried out using 1:300 scale orthophotos, which facilitated their identification. The quarries were then visited in the field, photographed, and documented in terms of their dimensions, depth, extraction methods, presence or absence of stonemason marks, vegetation cover on the cut surfaces, and granite type. All this information was compiled into a database, the records of which are held by the Gran Duque de Alba Institution.

The tourist route was designed around quarries and geological mesostructures located near the unpaved road connecting Cardeñosa and the Castro de Las Cogotas. One quarry was selected for each granite type used in the monuments of Ávila, provided it displayed notable features of its exploitation—ancient and modern, where applicable—and allowed observation of changes in quarry dimensions and cutting techniques over time. Significant archaeological elements were also included, such as pre-Roman wedge marks and remnants of millstone extraction. Geological points of interest were concentrated in the Cogotas area due to its well-exposed outcrops and the abundance of atypical mesostructures.

A total of 14 thin sections were extracted from the various granite facies of the Cardeñosa-Cogotas area to conduct petrographic observations. Although this study's itinerary includes visits to ancient quarries, we have chosen to collect samples from contiguous modern quarries for two reasons: (i) to avoid damaging the historic quarry, and (ii) to characterize the granitic lithotype without traces of weathering. The observations detailed herein focused on the texture and differentiation of the rock-forming minerals present in the granite. The thin sections, with a thickness of 30 µm, were prepared by the Servicio de Preparación de Rocas of the University of Salamanca. The petrographical study was performed using a LEITZ, Larbolux 12 Pol S polarized optical microscope. This instrument was also employed to ascertain the calcium content in plagioclase (anorthite component) by means of the Michel-Levy method. Modal calculations for volumetric mineralogical analysis were performed on the 14 thin sections using the traditional SWIFT brand counter from Basingstoke (UK). The step size was modified based on the grain size of the granite according to the Asociación Española de Normalización (UNE-EN 12407, 2020). The total number of points for each sample was determined to be 2,000. Petrographic observations and modal calculations were carried out at the Petrology and Geochemistry Section of the Geology Department of the University of Salamanca.

A series of rigorous chemical analyses were performed to achieve two objectives: first, to characterize the granite types; and second, to obtain constraints about their petrogenesis. Following the petrographic study, a total of 11 samples were selected from the 14 thin sections collected for petrographic study, on the basis of the absence of weathering. The 11 samples encompass all of the area's granite types. Chemical analyses were carried out at ACTLABS, Ancaster (Canada), using the 4LITHORESEARCH package to determine the major elements from the quarries by ICP-OES and the trace elements by ICP-MS. Additionally, 4 samples of monuments were analyzed in the same laboratory using the 4B package.

Thermometric conditions were constrained by the saturation of zircon (Watson and Harrison 1983), and the Al-Ti geothermometer (Jung and Pfänder 2007). Geobarometric constraints were executed in accordance with established estimates and empirical investigations within the Qzt-Ab-Or haplogranite system, as previously delineated by Tuttle and Bowen (1958), Luth et al. (1964), and Ebadi and Johannes (1991). To this end, mineral associations within the context of contact metamorphism were also utilized. Initial water content of granite melts was estimated from the F (Fe+Mg+Mn)-An-Or pseudoternary plot of Castro (2013), including cotectic lines obtained from experimental work in tonalite-granodiorite suites. Magma water content at the crystallization conditions was estimated from the empirical model based on the H_2O (vapor)=H_2O (melt) equilibrium of Moore et al. (1998) for an XH_2O in vapor of 1, using the H_2OSOL.X1 module for Excel, provided by Gordon Moore. The fugacity of water was also estimated using the H_2OSOL.X1 module, which uses the MRK equation of state and the calculation routine of Holloway and Blank (1994). The comprehensive array of data was input into the Metales Críticos database (López-Moro et al. 2023), a platform that facilitates the calculation of chemical-mineralogical, geochemical, and geothermobarometric parameters.

Results and Discussion

Geological Mapping of the Cardeñosa-Cogotas Area

A detailed cartography carried out of the Cardeñosa-Cogotas area reveals five mappable granitic facies (Fig. 3A), as well as a non-mappable hybrid facies located near the Las Cogotas dam. The mappable facies are listed below: porphyritic coarse-grained biotite granite (commercial name today "Gris Cardeñosa") (PCBG), fine-to-medium-grained inequigranular biotite granite (FMIG), a fine-grained biotite

granite (FBG), a fine-grained biotite granite with nodules (FGN), and a fine-to-medium equigranular two-mica ± tourmaline granite (commercial name today "Rubio") (TMTG) (Fig. 3A). These facies manifest in the monuments of Ávila, though the granite porphyry dikes utilized in the wall of Ávila are absent among the fresh rocks in the Cardeñosa-Cogotas area, a material that was extracted from the dikes themselves and that outcrops in the city of Ávila (López-Plaza 2024). The mapping also reveals that FBG is the most abundant, followed by PCBG, TMTG, FMIG and finally, the FGN, which is very scarce except for the area near the Las Cogotas dam. In addition, the distinction between the FGN and the FBG can be challenging to discern in outcrops, unless there are quarries that permit the observation of the fresh rock. The mapping also reveals that the previous mapping of the area, which only reflected 2 granitic facies, was inaccurate.

Location and Distribution of Quarries

A total of 255 quarries have been identified in the Cardeñosa-Cogotas area, 46% of which are ancient and 54% are more recent (Fig. 3B). Ancient quarries are considered to be those with abundant vegetation in the cutting planes, remains of wedge slots, and shallow workings. The ancient quarries are distributed across virtually all granitic facies, which aligns with the use of these granitic facies in monuments in Ávila and other nearby locations. The FBG, comprising 46% of the total, and is the granitic facies with the highest number of quarries. This is followed by the PCBG (34%), the FMIG (15%), the TMTG (4%), and FGN (1%). It is notable that the TMTG is used infrequently in traditional quarrying in this region, despite its comparable area to that of the FMIG. Additionally, the scarcity of the TMTG is evident in the limited presence of this granite facies in the monuments of Ávila.

In the Cardeñosa-Cogotas area, the extraction of granite by both ancient and modern stonemasons has been so significant that the granitic boulder has been largely removed, with the most notable impact observed in granitic facies such as the FBG. The historical quarries and a significant portion of the more contemporary ones are relatively modest in scale. The historical quarries are primarily superficial, and in most cases, contain a considerable amount of waste material that was not utilized by the stonemasons. The quarrying activity has been intense, with the same spaces being used during several periods on numerous occasions. Consequently, it is very common in recent quarries to find remains of traditional quarrying (e.g., wedge slots) in superficial areas and remains of modern quarrying in deeper areas of the fronts. In general, surface boulders or outcrops with slopes that allow the extraction of granite were exploited, as this was a methodologically challenging process in other scenarios.

Macroscopic Characterization of Main Granite Types

The most salient macroscopic characteristics of the five granite facies from the Cardeñosa-Cogotas are enumerated below. The PCBG is a light gray granite that exhibits a granular appearance, with a coarse-to-medium grained, and sometimes porphyritic texture due to K-feldspars megacrysts (Fig. 4A). At the outcrop scale, this granite exhibits significant variations in its composition and texture. It is characterized by the presence of numerous mafic microgranular enclaves (MME) (Fig. 4A), exhibiting a range of compositions from dioritic to granodioritic (IGME 1982), with a preponderance of tonalitic types. Additionally, there is a proliferation of small aplitic and pegmatite dykes in the apical zone forming a network, but also typically exhibits angular blocks in stoping zones, banded structures, and magmatic breccias. In some cases, PCBG is arranged as roof pendants or macroenclaves above the TMTG. This granite frequently displays mineral alignment.

The FBG is a fine-grained granite that is characterized by its high degree of homogeneity. It exhibits a grayish hue when fresh (Fig. 4G), and its color transitions to ochre when exposed to weathering. The granite typically exhibits reddish patinas of Fe oxides on the surfaces that are exposed to weathering. The presence of a high degree of fracturing is a distinguishing feature of the FBG, giving rise to a staggered morphology with small parallelepipedal blocks arranged in the form of grades. In the roof zones, the formation of biotite-rich layers is frequently observed. This granite is notable for the absence of enclaves or differentiated minerals, with the exception of a few instances where megacrysts of potassium feldspar with an envelop of biotite have been identified. These crystals correspond to fragments of the PCGB.

The FGN is found in close proximity to other granitic types and manifests as small outcrops that are rarely mappable. It's a fine-grained granite whose mesoscopical appearance is analogous to that of the FBG and it is considered to be as a subfacies of the preceding granite. However, it is distinguished by its finer grain size and the presence of nodules of ferromagnesian mineral aggregates (Fig. 4J). A distinctive feature of this granite facies is the presence of tourmaline-rich miarolitic cavities at various levels.

The TMTG is a fine-to-medium-grained leucocratic granite with a yellowish hue, resulting from a homogeneous superficial alteration that penetrates a minimum of 2 m and partially oxidizes the mafic minerals, altering the feldspars,

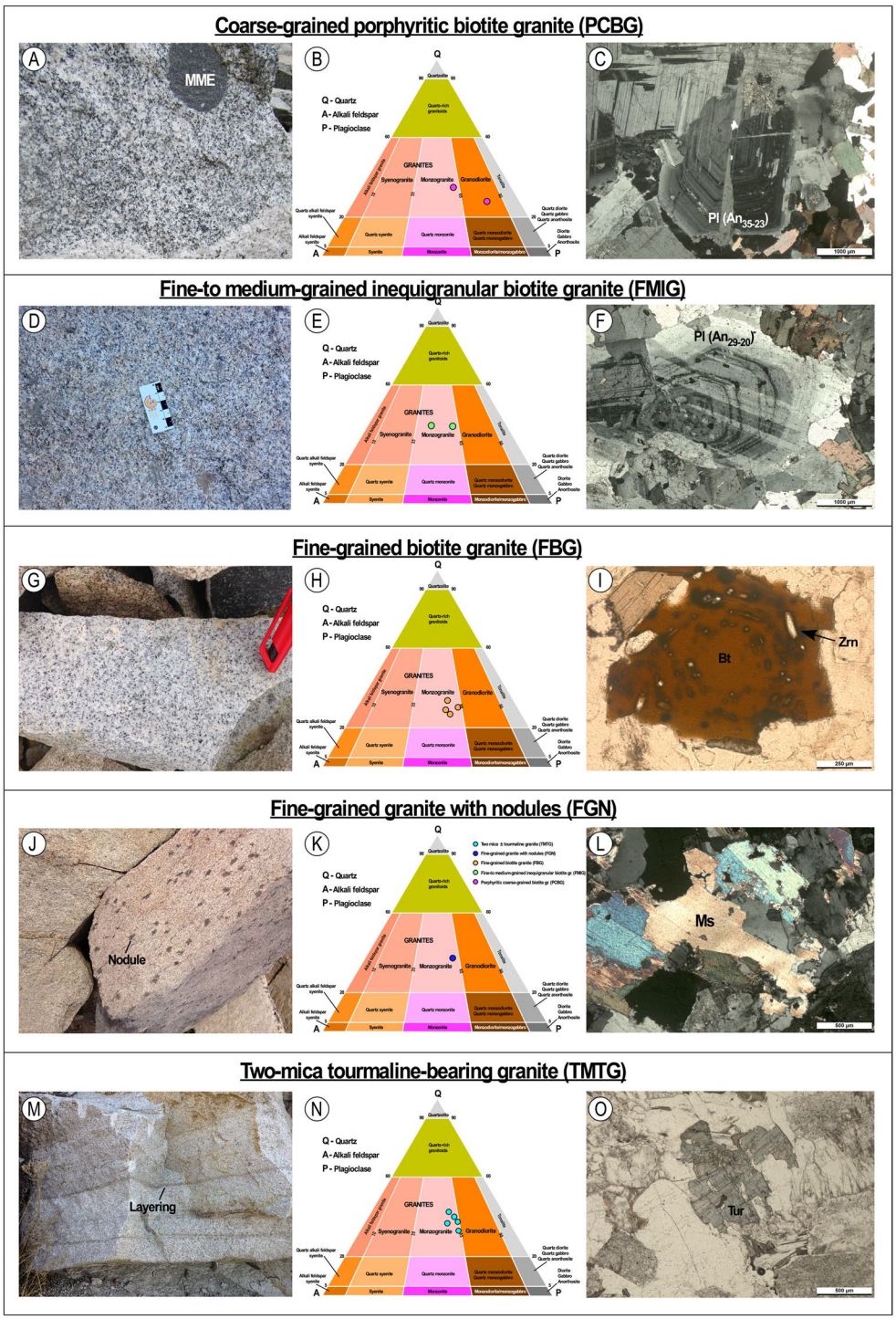

Fig. 4 Granite type characterization. The images on the left side of the figure illustrate the primary mesoscopical characteristics of each granite type. The images in the center of the figure represent the modal classification plotted onto the QAP ternary diagram. The images on the right side of the figure depict the distinctive petrographic features of each granite type described in the text. MME: mafic microgranular enclave; mineral abbreviations after Warr (2021)

particularly the potassium feldspar. Variations in grain size, the proportion of micas, the presence of small enclaves, and mica layers are possible (Fig. 4M). The enclaves are rare, small in size, and compositionally rich in biotite or aggregates with quartz, plagioclase, cordierite, and biotite. In some cases, these granite bodies exhibit miarolitic cavities, characterized by the presence of large crystals of potassium feldspar and/or quartz.

The FMIG and the PCBG display analogous morphological characteristics, though the size of the former's boulders is comparatively smaller. The disparities between these two facies manifest most distinctly in their characteristics pertaining to texture, composition, color, grain size, and the prevalence of enclaves. The FMIG exhibits a slightly porphyritic character, fine to medium grain size, and light gray color with minimal bluish hues and rare MME (Fig. 4D).

This may have influenced the extensive and preferential exploitation of the FMIG over the PCBG.

Sequence of Emplacement

This is a pivotal element in the interpretation of certain mesostructures with a high geotourist potential (see below). In the absence of radiometric ages, the sequence in which the different types of granite in the area were emplaced has been established using a range of mesoscopical criteria. These include contact relations (granite cutting other granite is younger), straight or warped margins (the latter indicating coevality, whereas the granite with a straight margin is early), the presence of engulfing blocks of granite that were emplaced earlier and are therefore colder, or differences in deformation, with the earlier granite being commonly the most deformed. The earlier facies to be emplaced was the PCBG, as is frequently found in angular blocks surrounded by other later granitic facies. It is commonly accepted that these angular blocks were in a cold state when they were enveloped by other granitic facies (American Geological Institute 1957); otherwise, they would not have retained their angular shapes and straight margins, but would have been warped and exhibited signs of mingling between the different magmas. The presence of TMTG and FBG dykes, characterized by well-defined straight margins, within the PCBG further suggests that the PCBG was already in a state of significant coldness when the dykes of other granitic facies were intruded. The coeval nature of the FGN and TMTG is further substantiated by the presence of synplutonic dykes with warped edges in the two-mica granite. These dykes have been observed in the FGN, indicating that at the time of TMTG intrusion, the FGN had not yet undergone its final solidification. In contrast, the FMIG is considered to be subsequent to the PCBG, as the contacts between these two formations exhibit a relatively linear disposition. The relationship between the FGN and the FBG remains to be elucidated. The mapping reveals that the TMTG is subsequent to the FBG (Fig. 3A), as the former is observed in dikes within the latter.

Petrographic Characterization

Fresh granites are distinguished by their texture, mineralogy, and mineral proportions. The PCBG consists of plagioclase (47−33% in vol.), quartz (29−23% in vol.), K-feldspar (22%−12% in vol.) and biotite (18−15% in vol.) as primary minerals. Accessory minerals (<5% in vol.) are muscovite, apatite, zircon, ilmenite, allanite, cordierite, and amphibole. The PCBG is classified in the QAP ternary diagram as monzogranite to granodiorite (amphibole-bearing facies) (Fig. 4B). It should be noted that the plagioclase has an oscillatory zoning, with a core up to An_{35} (andesine) and more sodic rims (An_{23}, oligoclase) (Fig. 4C), and in the amphibole facies there are reabsorbed cores. Also noteworthy are biotite crystals up to 2.8 mm with a plethora of apatite and zircon inclusions. The amphibole facies shows amphibole clots associated with biotite.

The FMIG is characterized by the presence of quartz (34−33% in vol.), plagioclase (31−24% in vol.), potassium feldspar (28−20% in vol.), and biotite (14−10% in vol.) as the primary mineral constituents. Accessory minerals include muscovite, cordierite, apatite (0.3−0.2% in vol.), zircon, ilmenite, and monazite. It is classified as monzogranite in the QAP diagram (Fig. 4E). Plagioclase manifests in crystals with dimensions reaching up to 5 millimeters, exhibiting pronounced zoning characteristics, featuring an oligoclase core (An_{29}) and a less calcic rim (Fig. 4F).

The FBG consists of plagioclase (41−34% in vol.), quartz (33−26% in vol.), K-feldspar (29−23% in vol.), and biotite (maximum 5.7% in vol.) as the primary mineral constituents. The presence of accessory minerals, such as muscovite (1.9−0.3% in vol.), biotite, apatite (0.3−0.2% in vol.), zircon (0.2–0.3% in vol.), ilmenite, monazite, rutile, allanite (0.2% in vol.), fluorite, and titanite, is also noted. It is a monzogranite in the QAP diagram (Fig. 4H). The felsic minerals approach 2 mm in size, with biotite being somewhat less (1 mm) and plenty of zircon, monazite and apatite inclusions (Fig. 4I). Plagioclase exhibits normal zoning, with altered core, which explains the frequent altered or dissolved plagioclase crystals in either outcrops or monuments.

The FGN, is characterized by the presence of circular aggregates, with abundant chlorite, pinnitized cordierite, quartz, and feldspars. The mesostasis is composed of quartz (36% in volume), plagioclase (35% in volume), and K-feldspar (23% in volume), as essential minerals. The presence of accessory minerals, such as biotite (3.1% in volume), muscovite (1.9% in volume), apatite, zircon, and monazite, further enhances the mineralogical composition. It is a monzogranite in the QAP diagram (Fig. 4K), with plagioclase classified as oligoclase in the core (An_{20}) and albite at the rim (An_{09}) and muscovite crystals close to 1 mm (Fig. 4L).

The TMTG is an equigranular, fine-to-medium-grained, two-mica ± tourmaline granite, with plagioclase (39−31% by volume), quartz (39−30% by volume), potassium feldspar (25−21% by volume), and muscovite (7.5–5.6% by volume) as the essential minerals. The accessory minerals are biotite (4.5−0.3% by volume), tourmaline (1.3–1.2% by volume), apatite, zircon and titanite. It is a monzogranite on the QAP diagram (Fig. 4N). Plagioclase is always albite. Tourmaline can reach 1.2 mm and occurs in isolated crystals (Fig. 4O).

Geochemical Characterization of the Granite Types

Compositionally, all samples are classified as granites (Fig. 5A), with silica contents ranging from 67.74 to 74.56 wt%, exhibiting the lowest values in the PCBG and the highest in TMTG (Fig. 5A; Table 1 S). The PCBG samples exhibited the highest concentrations of MgO, MnO, Fe_2O_3t, CaO, and Al_2O_3, as well as the highest values in the Larsen Index (i.e., $1/3SiO_2+K_2O$-(FeO+MgO+CaO); Larsen 1938), the Solidification Index (i.e., MgO×100/(FeO+Fe_2O_3+MgO+Na_2O+K_2O); Kuno 1960), the B parameter (i.e., Fe+Mg+Ti in millications; Debon and Le Fort 1983) and the modified alkali-lime index (MALI, i.e., Na_2O+K_2O-CaO; Frost et al. 2001) (Table 1 S). These variations can be attributed to the high biotite modal content, the low quartz abundance, the substantial Ca budget of its plagioclase and occasional amphibole occurrence. All quarry granites exhibit peraluminous character, with the

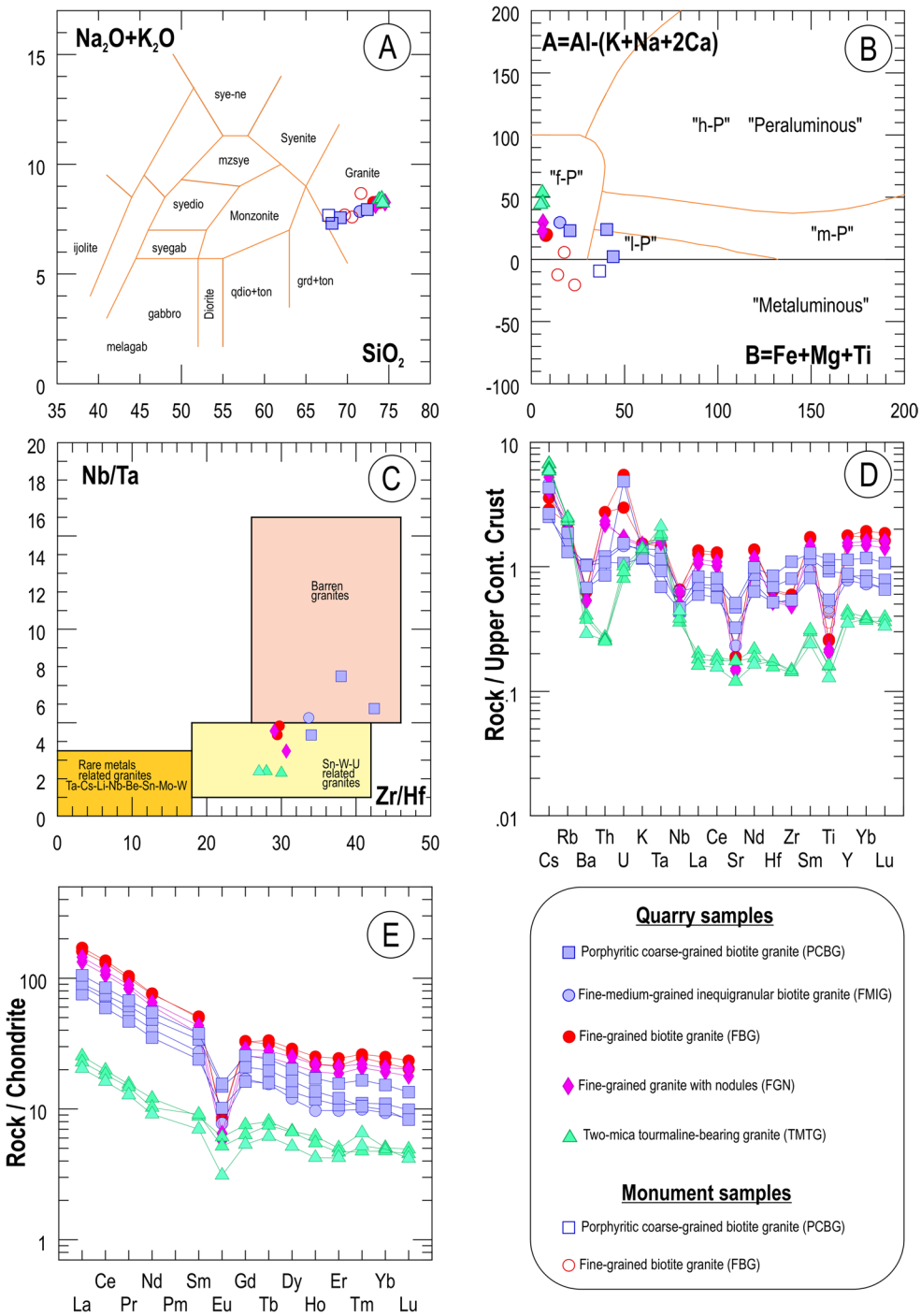

Fig. 5 Geochemical constraints. (**A**) Classification diagram of Cox et al. (1979). (**B**) A-B multicationic plot of Debon and Le Fort (1983), modified by Villaseca et al. (1998). L-P: low peraluminous; m-P: moderately peraluminous; h-P: highly peraluminous; f-P: felsic peraluminous. (**C**) Evolution of Nb/Ta as a function of Zr/Hf from Ballouard et al. (2016). (**D**) Spidergram normalized to the upper continental crust from Taylor and McLennan (1985). (**E**) REE patterns normalized to the chondrite from Sun and McDonough (1989)

highest values observed in TMTG and FGN, as they contain the higher proportion of Al-rich minerals, such as muscovite and tourmaline. Furthermore, the high biotite content in PCBG triggers the low value in the A/CNK index [i.e., $Al_2O_3/(CaO+Na_2O+K_2O)$].

In contrast, monument samples exhibit a metaluminous character, despite sharing the same facies as quarry samples. This results in parameters such as the A (i.e., Al-(K + Na + 2Ca) in millications; Debon and Le Fort 1983) being negative (Fig. 5B). This variation can be attributed to the presence of higher levels of alkalis, particularly calcium (Ca) and sodium (Na), in the monument samples (Table 1 S). This increase in alkali content can be attributed to the dissolution of mortars present within the monument, which subsequently precipitate within the small cracks present in the ashlars (Arnold and Zehnder 1989).

LIL elements such as Cs and Rb, due to their incompatible nature in a melt, are more abundant in more evolved granites, particularly the TMTG (Fig. 5D). Conversely, Ba is significantly depleted in this granitic type (Fig. 5D) due to the scarcity of biotite and potassium feldspar, minerals with the highest mineral/melt partition coefficients in granitic melts (Pichavant et al. 2024). With respect to high field strength elements (HFSE), those that are strongly accommodated in monazite, such as Th, Y, and REE, especially LREE, are more enriched in facies containing biotite replete with microinclusions, including monazite, such as FBG and FGN (Figs. 4I and 5D and E). Conversely, TMTG, characterized by its limited biotite and scarcity of microinclusions, exhibits a notable depletion of these elements, a hallmark of geochemical characteristics exhibited by highly evolved granites with minimal monazite presence. Furthermore, Zr and Hf demonstrate strong accommodation in zircon, with comparatively lower proportions present in allanite, rutile, amphibole, and likely biotite (see https://earthref.org/KDD-old/). Given the prevalence of these accessory minerals in the PCBG and its status as the most biotite-rich granite facies, it is the granitic type with the highest content in Zr and Hf (up to 208 µg/g of Zr and 4.9 µg/g of Hf). In contrast, the TMTG, due to the scarcity or absence of these minerals, exhibits the lowest concentrations. Another intriguing HFSE pair is Nb and Ta, which are notably accommodated within columbite or pyrochlore group minerals, but absent from all granite samples examined. These elements are also fractionated by rutile, ilmenite, biotite (Nb and Ta), and muscovite, though the latter exclusively accommodates Nb (Pichavant et al. 2024). Typically, Nb and Ta are incompatible elements in an igneous system and tend to concentrate in the most evolved granitic melts. Therefore, it is expected that their concentrations will increase from PCBG to TMTG, a process that occurs in Ta but not in Nb. This discrepancy is likely attributable to a strong fractionation of biotite, muscovite, and ilmenite, which strongly fractionate Nb against Ta (Pichavant et al. 2024). Consequently, this results in a decrease in the Nb/Ta ratio (Fig. 5C).

Isovalent trace elements as Nb, Ta, Y, Ho, Zr and Hf and the lanthanide tetrad effect may be used to decipher whether geochemical twins as Zr-Hf, Y-Ho, or Nb-Ta show chondritic ratios (CHARAC behavior), typical of pure silicate melts, or non-chondritic behavior as a result of fractionation in aqueous media or in high-silica magmatic system enriched in water, Li, B, F, P and Cl. In the present case, all Zr/Hf (27–42.5.5) and Y/Ho (25–32) ratios are chondritic (i.e., 26–37 and 27–38, respectively, see Irber 1999), but the low values (<5) of Nb/Ta ratios (Fig. 5C) along with the values observed in the tetrad effect of the REE ($TE_{1,3}$>1.1, Table 1 S) in the TMTG, are indicative of an evolution with participation of fluxing elements, in this case Boron. In a similar fashion, the Nb/Ta-Zr/Hf diagram demonstrates that, except for PCBG and FMIG, the remaining granites are Sn-W-U related (Fig. 5C).

Temperature of Crystallization of Granite Melts

Zircon saturation temperature and Al-Ti thermometer data indicate that PCBG and FMIG were the granite magmas that crystallized at the highest temperature (886–776 °C and 802–755 °C, respectively, Table 1 S and 1). These were followed by FBG (760–738 °C) and FGN (747–714 °C), with TMTG (664–663 °C) being the granite that clearly crystallized at the lowest temperature (Table 1 S and 1). The low temperatures of TMTG are probably due to its abundant content of a fluxing element, such as boron, accommodated in the tourmaline mineral. This flux element is capable of lowering the temperature of a granitic magma to a remarkably low range of 570 to 600 °C for 17% B_2O_3 (Pichavant 1981). This phenomenon stands in striking contrast to the crystallization process of granitic melts that contain only water, which occurs at temperatures ranging from 715 to 725 °C (Tuttle and Bowen 1958).

Geobarometry of Emplacement of Granite Melts

The Qzt-Ab-Or ternary diagram was utilized to constrain the emplacement pressure of the granites under study, employing a combination of cotectic lines and compositions of H_2O-saturated minima and eutectics. This methodology is exclusively applicable to final evolved melts, namely the TMTG, the FGN, and the FBG, which are plotted between the 100 and 200 MPa cotectic lines (Fig. 6A). Furthermore, the PCBG triggered contact metamorphism with cordierite and andalusite (IGME 1982), which may be used to estimate the pressure conditions of the emplacement of this granite facies. The blastesis of cordierite and andalusite in the absence of chloritoid, which has not been cited in the

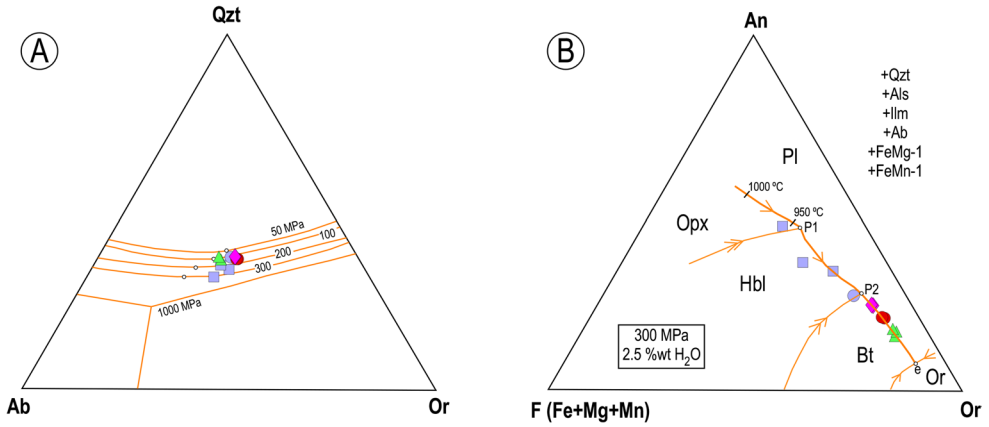

Fig. 6 (**A**) Cotectic lines (orange lines), eutectics, and water-saturated minima (white circles) in the Qzt-Ab-Or ternary plot for different pressures. Data from Tuttle and Bowen (1958), Luth et al. (1964), and Ebadi and Johannes (1991). (B) F-An-Or pseudoternary diagram from Castro (2013), using as projection points Qzt, Al-silicate, Ilm, Ab and the exchange vectors $FeMg_{-1}$ and $FeMn_{-1}$. Cotectic lines, peritectic and eutectic taken from Castro (2013) for a pressure of 300 MPa, an initial water content of 2.5 wt% and a primary magma of andesitic composition. The peritectic points are labeled P1 and P2, and the eutectic point is labeled e. In P1, Opx + Liq react to give Hbl, and in P2, Hbl + Liq react to give biotite. Symbols as in Fig. 5

contact aureole of these granites (IGME 1982), may be formed according to the following reactions: Mus + Chl + Qzt = Crd + Bt + vapor at 120–250 MPa and 500–550 °C; Mus + Bt + Qzt = Crd + Kfs + vapor at 150–250 MPa and 550–625 °C; and Mus + Qzt = And + Kfs + vapor at < 350 MPa and 550–625 °C, suggesting pressure conditions close to 250–300 MPa for the PCBG facies. A notable observation is the striking similarity between these values and those depicted in the Qzt-Ab-Or diagram.

Water Content of Granite Melts

The initial water content of granite melts was estimated by comparing the composition of the samples with the cotectic lines obtained experimentally for granodiorite melts plotted in the F–An–Or pseudoternary diagram from Castro (2013) (Fig. 6B). The majority of the samples exhibited a high degree of compatibility with the cotectic line of a water-undersaturated melt, with a water content of 2.5% and a pressure of 300 MPa, and an andesitic melt serving as the initial starting point (Fig. 6B). Therefore, the present study establishes an initial water content of 2.5% as a baseline for all granite types. This finding aligns with the observed congruence with the cotectic line in Fig. 6B, thereby substantiating the hypothesis of cogenetism among all the studied samples. It is important to note that as a granitic melt cools, its water content increases due to the precipitation of predominantly anhydrous minerals and the ability of the melt to dissolve more water at lower temperatures (López-Moro et al. 2024). This is the rationale behind the assessment of the water content and fugacity of water (fH_2O) at near-crystallization conditions for each granite type (see Table 1 S and 1). The PCBG exhibited the highest water content (up to 7.25%, average 6.97%), and the FMIG had the lowest water content (5.04%) (Table 1 S). In relation to fH_2O, a parameter that quantifies the propensity of water to escape from the system influenced by its activity and interaction with other components of the magma, the values obtained range, on average, from 242 MPa in the PCBG to 98 MPa in the TMTG (see Table 1 S and 1).

Structural Constraints: Blocometry of the Granite Types

Cutting a stone as hard as granite to produce ashlars is not without difficulty, since the granite must have some kind of mineral orientation (fabric) or microcracks. In the absence of these planes, the rock breaks in conchoidal planes or generates non-uniformly split blocks, resulting in blocks that are not suitable for the production of ashlars. In the Cardeñosa area, not all the granitic facies have this orientation, and their presence or absence is related to the chronology of the emplacement of each of them. Thus, the granitic facies that were emplaced first are the ones that best show this mineral orientation (e.g., PCBG), which is not observed, or to a much lesser extent, in the later facies (e.g., TMTG). This mineral orientation, when visible in the Cardeñosa area, has a direction close to N-S, which is why the stonemasons of the area refer to this orientation as “the North” (or local direction of grain plane). The importance of this structural characteristic is such that it probably determined the scarcity of the use of very poorly oriented granites, such as the TMTG, in the monuments of Ávila.

The extraction of granite blocks from the Cardeñosa area was also strongly controlled by the presence of fracture planes without displacement between blocks (joints), which

usually occur in families. The most common in the area is to find 2 or 3 families of subvertical or with angles close to 45°, plus a family of subhorizontal planes. The genesis of the subvertical families is essentially related to tectonic processes of the granitic magma, while the subhorizontal ones are due to the process of decompression and erosion of the rock mass, which generates a stress regime that tends to fracture the rock by planes parallel to the topographic relief (Hobbs et al. 1976). The subvertical joints in PCBG and FBG are usually very similar in direction, with two main orthogonal families, one N-20-E and the other tending E-W (Fig. 7A, C, D and F). In contrast, the TMTG, in addition to the two main subvertical systems mentioned above, displays a third family of directions: N-55°-E, with a dip of 52° to NW (Fig. 7G and I). The latter makes it difficult to obtain parallelepiped blocks, which, together with the lack of mineral orientation in this facies, has meant that it has not been mined in abundance in the area, although it is a much sought-after rock and appreciated for its characteristic whitish color. On the other hand, the spacing of the main join subvertical systems determines the size of the block that can be quarried, an aspect that the master stonemasons were well aware of in order to supply granite of one type or another according to the requirements of the

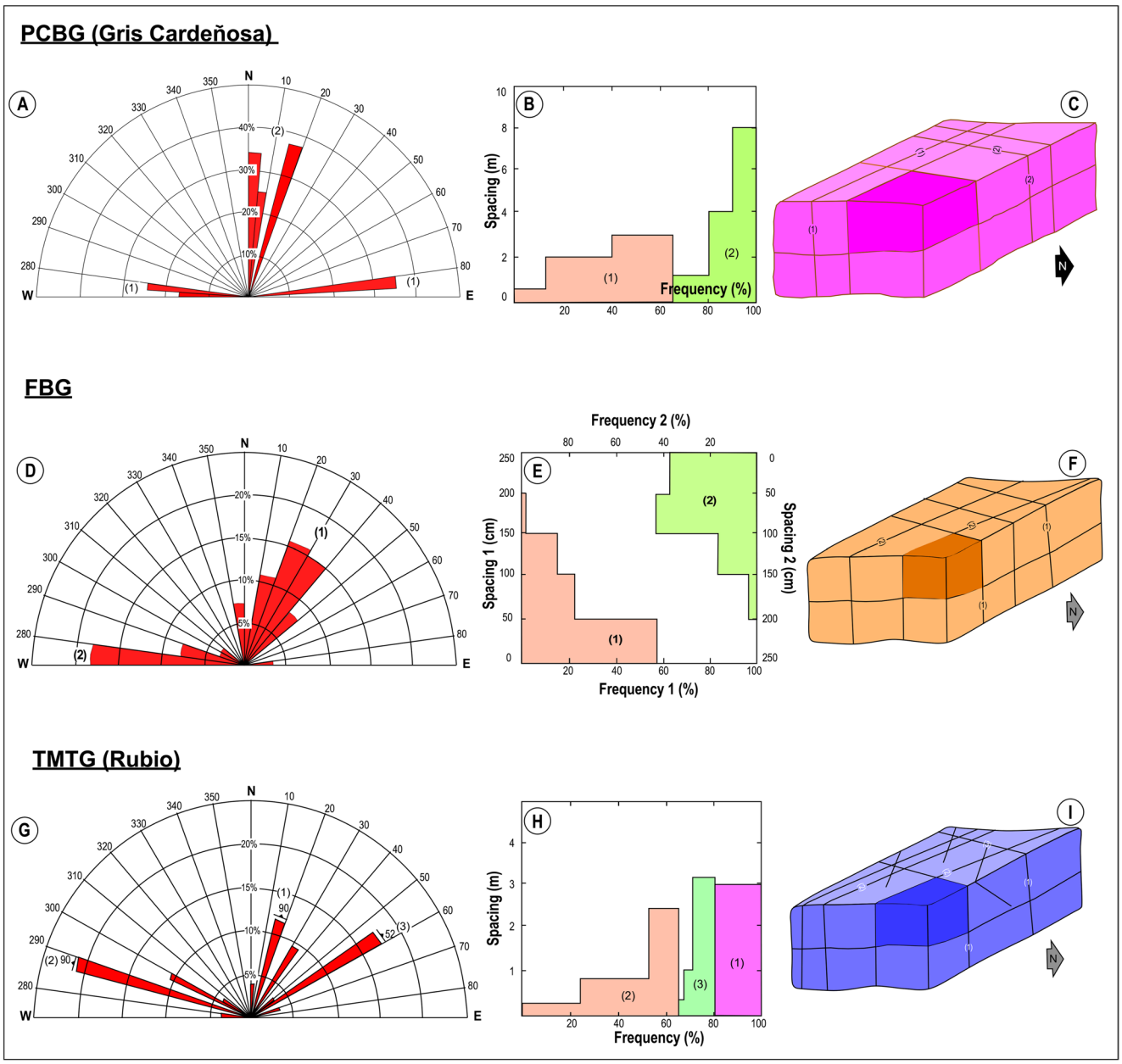

Fig. 7 Rose diagrams showing joint planes, histograms with joint spacings, and block diagrams with block size and shape

monuments. In fact, the join systems of the PCBG are all several meters apart (Fig. 7B), which makes it possible to quarry large blocks that are easy to split because of their very pronounced mineral structure. The FBG, on the other hand, has joint spacings of tens of centimeters, so the blocks are much smaller (Fig. 7E).

As for the subhorizontal joints (sheet joints), it has been observed that it is less spaced (tens of centimeters) in the first few meters and then it increases or disappears (Fig. 8A). The FBG have the smallest spacing, while the PCBG have the largest spacing. It is important to acknowledge the profound influence of these sheet joints on the traditional extraction methods employed in quarrying. This is primarily due to the impracticality of extracting blocks below ground level, which led to a very superficial working, based on the exploitation of granite boulders (Fig. 8B) and granite hills on a slope (Figs. 8C and D).

Evolution of Cutting and Quarrying Technology

The Cardeñosa-Cogotas area has been an important area for granite quarrying from the time of the "Vettons" to the present day, which a priori allows us to deepen our knowledge of the evolution of the quarrymen's cutting techniques. In fact, in the area of the hill fort of Cogotas, built by the "Vettons" in the Iron Age, it is the only site where we have found wedge slots of exceptionally large dimensions (up to 33 cm) (Fig. 9A). These wedge slots occur only in the PCBG, in rounded blocks that could have been used to make the famous Vettonian boars. In the surroundings of the hill fort, other types of granite, such as the FBG, do not have wedge slots, perhaps because they have narrow subhorizontal joints that allow the removal of small blocks with simple levers, making this rock the most used in the construction of the hill fort and its houses.

Outside the surroundings of the hill fort, in the oldest quarries, wedge slots of about 15–21 cm can be seen in all the granite types (Fig. 9B). In more recent quarries, the remains of wedge slots are all smaller than 10 cm, generally around 5 cm, being particularly small in the fine-grained biotite granites (Fig. 9C). Therefore, it seems obvious that there has been a reduction in the size of wedge slots over time. The reason for this evolution is not well known, but the use of 33 cm wedge slots could be related to the use of wooden wedges that would break the rock by traction by increasing their volume when wetted with water. These wedge slots are similar in size to those found in historic Egyptian granite quarries, which are thought to have been designed to accommodate wooden wedges (García de los Ríos Cobo 2018). The change from wedges of 15–21 cm to those of less than 10 cm could be due to an improvement in the quality of the materials used to make the wedges, but we do not know for sure.

The area under consideration also permits a comparison of quarry fronts of different ages, thereby enabling the establishment of a possible evolution of quarrying. In the earliest quarrying fronts, the extraction of rock was predominantly executed through the use of wedges, and the technological

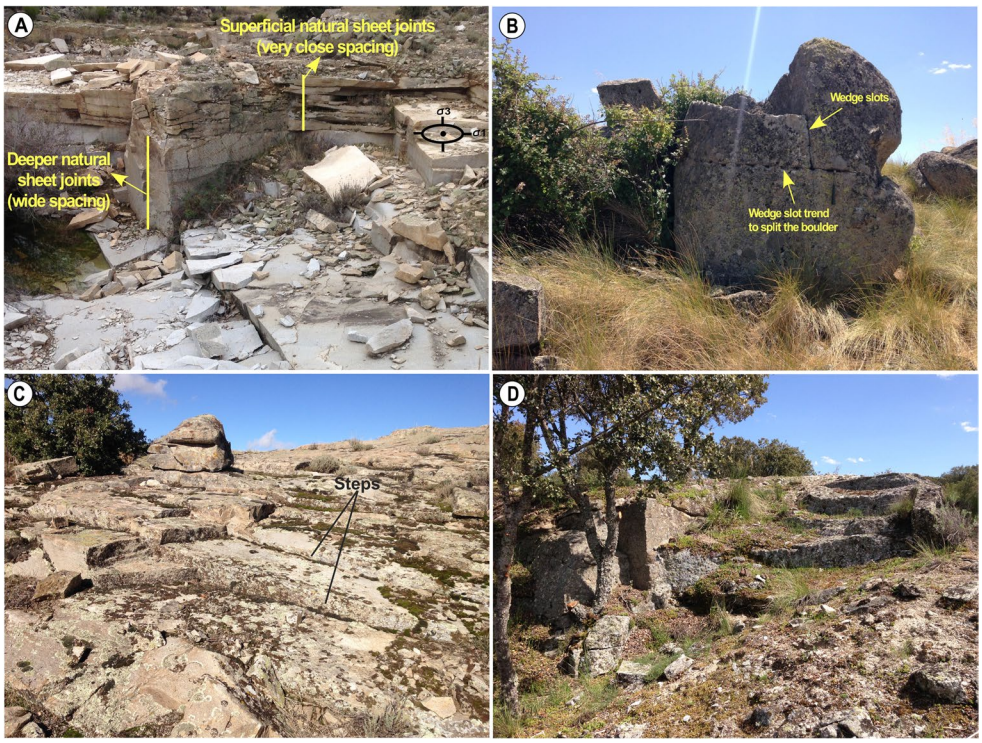

Fig. 8 (**A**) Distribution of sheet joints in the FBG, with very close spacing in the first few meters and wider spacing at depth. Two of the main axes (sigma 1 and sigma 3) of the stress ellipsoid are shown, corresponding to a non-hydrostatic stress resulting from load release due to erosion, which in this case breaks the rock into more or less subhorizontal planes. (**B**) Surface mining of a PCBG granite block using traditional methods. C and D) Fronts of historical quarries quarried on a slope using traditional methods, in FBG (**C**) and PCBG (**D**)

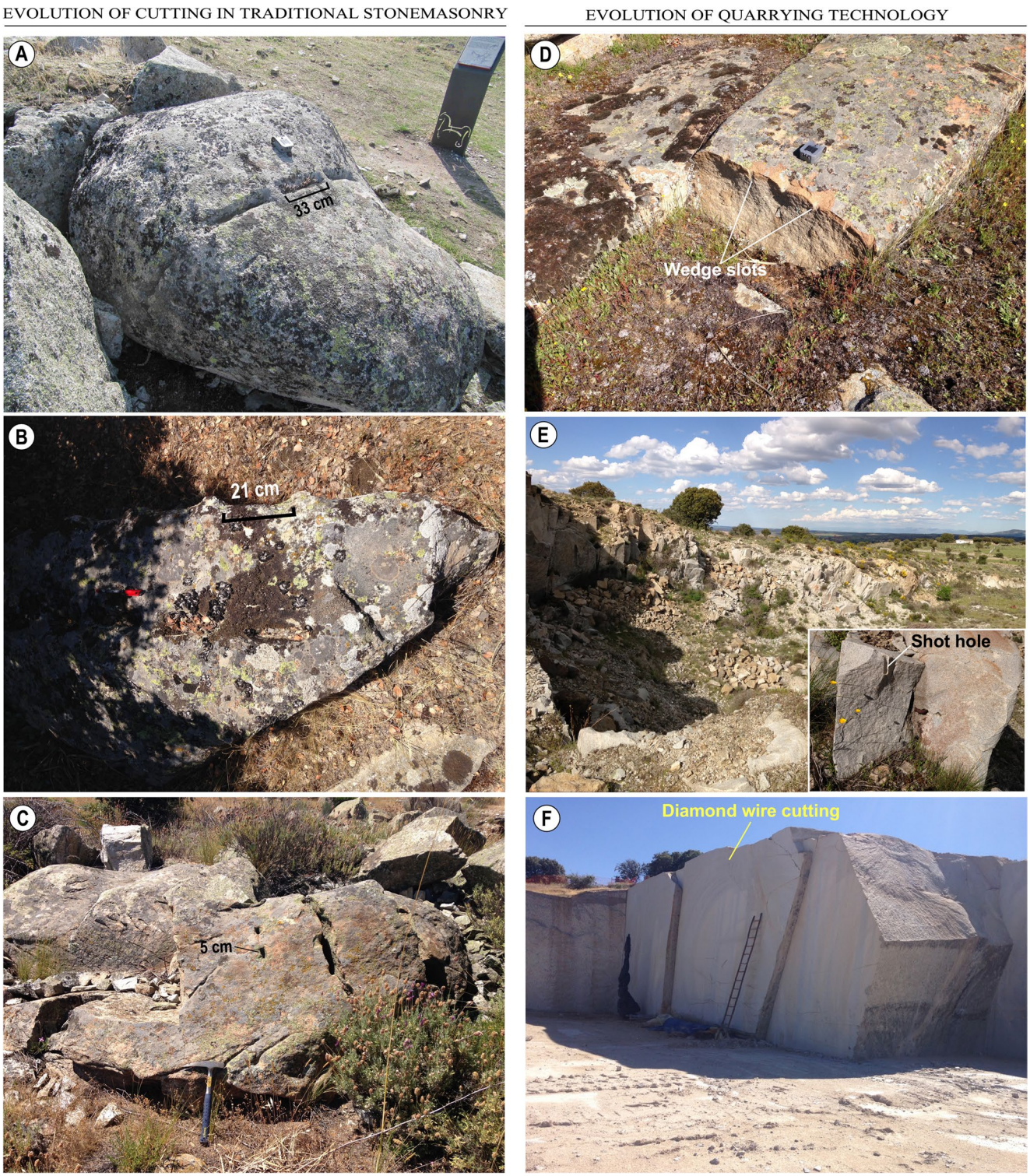

Fig. 9 A, B and C) Evolution of cutting in traditional stonemasonry in the Cardeñosa-Cogotas area. (**A**) Giant wedge slots (33 cm in size) in the PCBG close to the Cogotas hillfort of Vettons. The direction of these structures follows the regional planar fabric. (**B**) Wedge slot of 21 cm in size in the FBG. (**C**) Wedge slots of 5 cm in size in the FBG. D, E and F) Evolution of quarrying technology in the Cardeñosa-Cogotas area. (**D**) The extraction of stone in a diminutive historical quarry, wherein the cutting was carried out with wedges applied to a block of FBG. (**E**) Abandoned front of one of the largest quarries in the area, called El Puchero quarry. The inset shows a FBG block with the remains of a shot hole where explosives were placed. (**F**) Quarry currently active in the Cogotas area, exploited with diamond wire. Note the working depth (almost 4 m) and the perfect contours of the cuts

capabilities were limited to superficial processing, until the emergence of the first subhorizontal planar joints (Fig. 9D). Consequently, the quarries were characterized by their diminutive scale, their concentration within boulders and granite hills on slopes, and the proliferation of multiple fronts that disseminated throughout the area (see Fig. 3B), a phenomenon that resulted in the devastation of the characteristic granite landscape. In more recent fronts, the advent of shot holes (see inset in Fig. 9E) permitted the integration of explosives, thus facilitating more profound excavations. This technological advancement enabled the deepening of excavations and the augmentation of operational scope, culminating in the formation of extensive and deep quarries (Fig. 9E). Finally, in the most recent quarries, the use of diamond wire has been employed, enabling deep excavations and the extraction of massive blocks with precise contours (Fig. 9F).

Tourism Route

The findings from the preceding sections pertaining to the Cardeñosa-Cogotas granitic material supply area, with all its geological, cultural and archaeological singularities, permit the formulation of a tourism route that encompasses all these subjects. The proposed tourist route is located less than 15 km from the city of Ávila and comprises 13 points of interest (POIs) (Fig. 10A). Twelve of these are situated near the hillfort of Las Cogotas (Fig. 10B–D), with a maximum distance of 1.8 km between the farthest points. Access to these POIs is via an unpaved road suitable for cars, which branches off approximately 1.5 km before reaching the town of Cardeñosa, at a junction marked by a sign indicating the route to the hillfort (Fig. 10A). Most POIs are easily accessible and located close to the road. Those nearest the hillfort—particularly those adjacent to the backwater

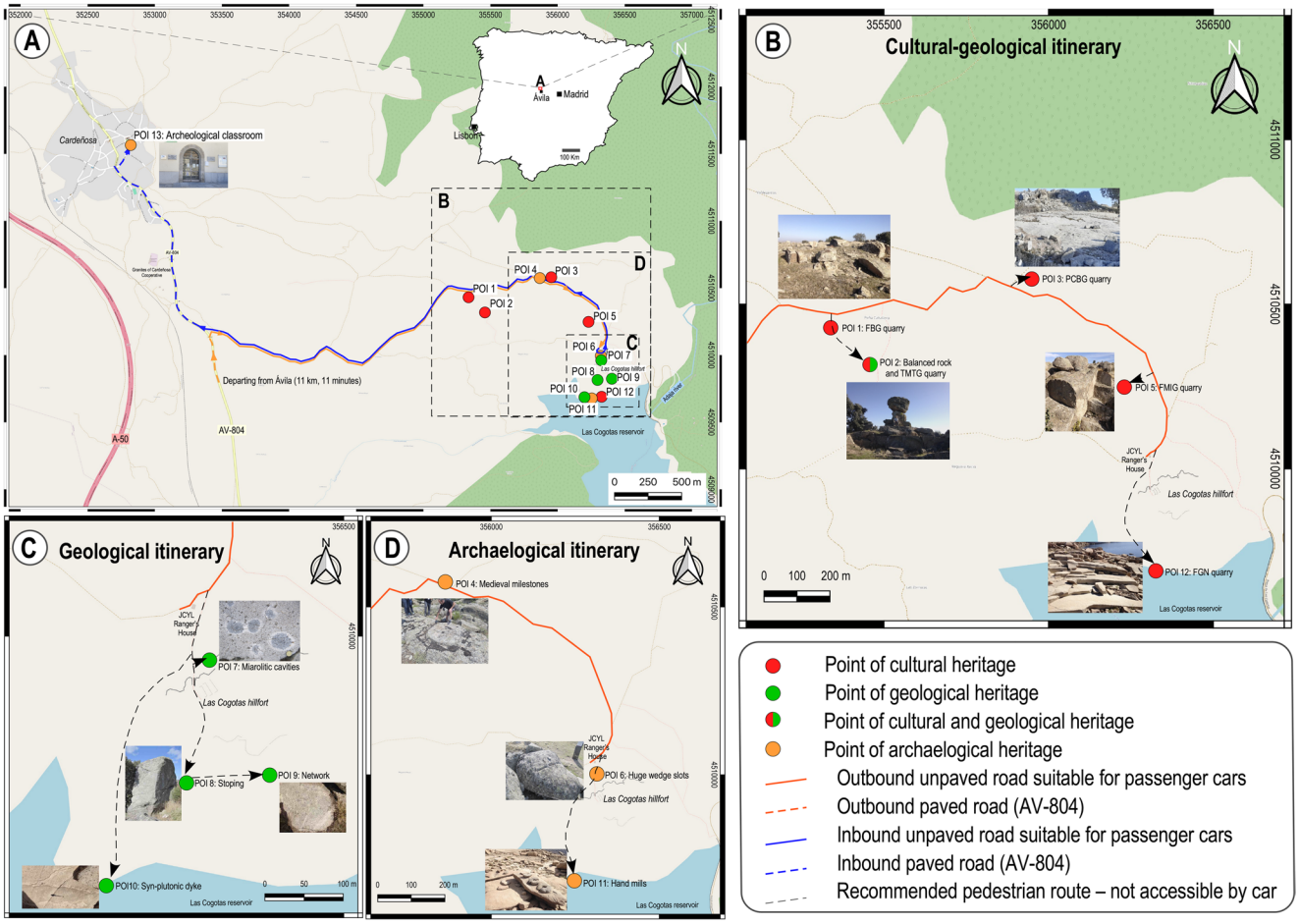

Fig. 10 Tourist route map with differentiated stops (POIs) of geological, cultural, and archaeological significance. (**A**) General overview of the tourism route, showing the suggested stops (POIs). The recommended sequence of visits follows the numbering assigned to each point of interest. (**B**) Detailed view of the route near the Las Cogotas hillfort, highlighting stops at historical quarries representing all fresh granite facies found in the monuments of Ávila. Note that some cultural POIs may also hold geological significance. (**C**) The same as in panel B, focusing exclusively on stops of geological interest. (**D**) The same as in panels B and C, showing stops of archaeological interest. Note that the archaeological itinerary ends at POI 13, which is included in panel A. Vector geographic base layer derived from OpenStreetView. Coordinate reference system: ETRS89/UTM Zone 30 N

area of the Las Cogotas reservoir—are somewhat more difficult to reach, occasionally requiring visitors to cross open fields. Nevertheless, they remain fully accessible to individuals without mobility impairments. These POIs may be submerged when the reservoir is at full capacity. POI 13, the final stop on the route, is located in Cardeñosa, directly opposite the church and approximately 5.5 km from the hillfort. Two route options are proposed. The first begins by parking near the JCYL ranger house at Las Cogotas and walking to the nearby POIs (e.g., 6–12, 5, 3, 4, 1, 2), followed by a drive to POI 13 in Cardeñosa. The second—and recommended—option starts at POIs 1 and 2, alternating between driving and walking (Fig. 10A), and ends at the ranger house, from which visitors proceed on foot to POIs 6–12 before driving to POI 13.

Additionally, three thematic itineraries—geological, cultural, and archaeological (Fig. 10B–D)—are available and can be followed using either route. The complete itinerary is designed as a one-day visit and can be completed in 5 to 6 h. The route presents no significant safety concerns. All quarries are small-scale, surface excavations with no risk of rockfall or collapse. Caution is advised near the reservoir backwater, particularly when visiting with children, to prevent accidental falls into the water.

Informational panels are available but focus exclusively on archaeological content. These panels are not related to the archaeological points of interest selected along our route. There is no doubt that our itinerary could serve as an incentive for the relevant authorities to commit to installing interpretive panels that would further promote tourism in the area.

The city of Ávila offers a wide range of restaurants and hotels, while the town of Cardeñosa, less than 5 km from the site, has up to three rural guesthouses. A detailed description of each Point of Interest (POI) is provided below.

Point of Interest 1: FGB Historical Quarry

This location (X: 355338.2, Y: 4510428.8; Lat. 40.732092°, Long. −4.713129°) is primarily of cultural interest, but it also provides a valuable opportunity for visitors to directly observe the FBG granite in situ. At this point of interest, the granite is exposed in ancient surface workings (Fig. 11A), allowing for close examination of its textural and mineralogical features. The main characteristics of this granite type are summarized in Table 1. The FBG has been a frequently utilized granite facies in the monuments of the city of Ávila, particularly during the Golden Age (Fig. 11B). The primary factors contributing to its extensive utilization in the Cardeñosa area are its substantial volume (Fig. 3A) and the relatively sparse spacing of its planes of diaclase (Fig. 7E and F) and sheeting (Fig. 8A), which facilitated its extraction by quarrying methods. However, its mineral orientation, which is not particularly pronounced in this facies, may have played a less significant role for extraction. At this Point of Interest, visitors can observe shallow workings, where broken blocks have been preserved, along with samples of wedge slots. A few meters away, visitors can observe more recent excavations that are deeper and utilize different cutting techniques.

Point of Interest 2: Balanced Rock and TMTG Historical Quarry

This location (X: 355458.8, Y: 4510318.1; Lat. 40.731116, Long. −4.711676) is of both geological and cultural interest (Fig. 10B). At this point, tourists may observe a typical form of erosion in granites, such as a balanced rock, together with one of the few old quarries of the TMTG granite in this area (Fig. 11C). A balanced rock is a naturally occurring geological formation featuring a large rock or boulder, sometimes of substantial size, resting on other rocks, bedrock, or a glacial till. Their origin is due to the differential decomposition and subsequent erosion of granite. The salient characteristics of the TMTG are delineated in Table 1, highlighting that it is the most evolved granite, emplaced and solidified at the lowest temperature of all granite facies and with a high volatile phase that it contains boron. The TMTG's utilization in the monuments of the city of Ávila (e.g., Fig. 11D) was negligible, presumably due to the granite's limited volume (Fig. 3A) and the challenges faced by the quarrymen in extracting it. These challenges include the absence of mineral orientation and unfavorable joints, resulting in the presence of a third, non-vertical, extraction-obstructing joint that impeded the extraction of squared blocks of significant size (see Fig. 7H and I, and Table 1). At Point of Interest 2, visitors have also the opportunity to observe several superficial ancient quarries. These quarries were likely utilized by quarrymen who capitalized on the presence of slight variations of height in terrain to extract granite blocks. In the vicinity of the balanced rock, it is also possible to observe some of the few parallelepiped blocks obtained in this lithology and with abundant wedge slots in their faces (see inset in Fig. 11C).

Point of Interest 3: PCBG Historical Quarry

This location (X: 355948.3, Y: 4510576.8; Lat. 40.733531, Long. −4.705941) is primarily of cultural interest (Fig. 10B), but it also offers a valuable opportunity for visitors to observe the PCBG granite in one of the most visually striking historical quarries within this granitic facies. This unit corresponds to the earliest emplacement phase and shows mild deformation, having crystallized under the

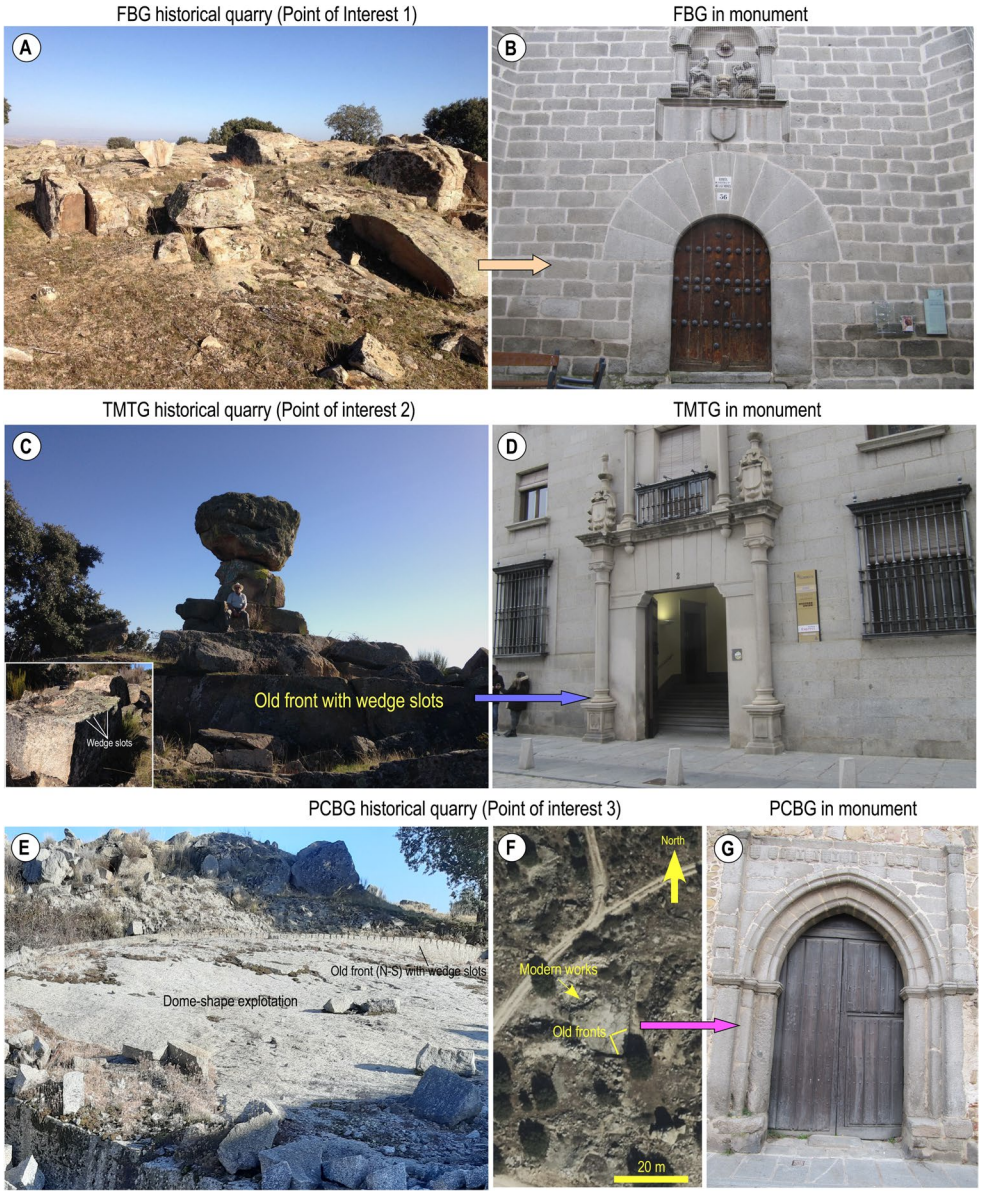

Fig. 11 Quarries and monuments of FBG, TMTG and PCBG. (**A**) Old surface workings in the FBG at Point of Interest 1. (**B**) Outside of the chapel of Las Nieves, built in the 16th century in the city of Ávila. The doorway of the building has been made with FBG. (**C**) Balanced rock and old quarry in the TMTG in Point of Interest 3. The inset corresponds to a parallelepiped block with abundant wedge slot marks in close proximity to the balanced rock. (**D**) Application of the TMTG on the façade of the Palacio del Rey Niño (current post office building). The 16th-century monument was mostly rebuilt in the 20th century by Clemente Oria, the municipal architect. (**E**) An old dome-shaped exploitation front with countless wedge slots in the N-S front in the PCBG. (**F**) Aerial photo showing the quarry in Photo E, with the two old fronts full of wedge slots following the direction of the joints (N-S and E-W) and mineral fabric (approximately N-S). There is also a smaller, more modern, and deeper front, where shot holes and explosives were used to cut the PCBG. Notice that the modern front is not in line with the direction of the joints. H) Gothic doorway of the Palacio de los Dávila (13th − 14th century), in the city of Ávila, made with the PCBG

relatively highest pressure conditions among the granites included in the itinerary (Table 1). The visitor will observe a dome-shaped exploitation front with innumerable wedge slots in two orthogonal cutting planes (Figs. 11E, and 11F), coinciding with the direction of the joint planes of this granite (compare Fig. 7A and C with 11 F). The extraction process was conducted up to the first natural dome-shaped joint, thereby unveiling a cupuliform hollow. As indicated by the available evidence, these represent the oldest workings. However, a few meters away, the visitor can observe deeper and more modern workings (see Fig. 11F). In these workings, drills have already been used to cut the rock. It should be noted that the modern front is not in line with the direction of the joints. The granite's substantial block size of PCBG, attributable to the notable natural spacing of its subvertical joints, in conjunction with its pronounced mineral fabric, which facilitated straightforward rock cutting, and the abundance of this granite facies, are reasons to the extensive utilization of PCBG from medieval times in monuments of the capital, Ávila (Fig. 11G), and the surrounding municipalities.

Point of Interest 4: Medieval Milestones

This POI (X: 355864.3, Y: 4510572.6; Lat. 40.733479, Long. −4.706934) is of archaeological interest (Fig. 10D). Visitors can observe an area where large millstones were extracted, or not completely extracted (Fig. 12A), for the

Table 1 Summary of petrological and quarry information of the granite types

Granite type	PCBG	FMIG	FBG	FGN	TMTG
Macroscopic and mesoscopical features	Porphyritic; MMEs-rich; network.	Inequigranular; MMEs-poor.	MGE-free; PCBG enclaves; reddish patinas; roof layers.	Crd nodules; miarolitic cavities.	Tur-bearing; roof layers; miarolitic cavities.
Sequence of emplacement	The first	After PCBG	After PCBG and prior to TMTG	Contemporary with of slightly earlier than FBNG	Contemporary with of slightly later than FBNG
Petrographical features	Pl (An_{35-23}); Bt (18−15%); Qz (29−23%); Amp clots.	Pl (An_{29-20}); Bt (14−10%); Cd-bearing.	Bt (5.7%); Qz (33−26%); Bt rich in inclusions.	Pl (An_{20-9}); Bt (3.1%); Ms (2%); nodules with Cd.	Pl ($An_{<10}$); Bt (1.2%); Ms (7.5%); Tur-bearing.
QAP classification	Granodiorite-monzogranite	Monzogranite	Monzogranite	Monzogranite	Monzogranite
Geochemical features (quarry)	Granite; L-P to f-P; the less evolved; barren granite.	Granite; f-P; intermediate composition between PCBG and other granites; barren granite.	Granite; f-P; high REE; Sn-W-U related granite.	Granite; f-P; high REE; Sn-W-U related granite.	Granite; f-P; the most evolved; low REE; Cs-Rb-B-rich; TE1.3 > 1.1; Sn-W-U related granite.
Geochemical features (monument)	Metaluminous; Na-Ca-rich	-	Metaluminous; Na-Ca-rich	-	-
Temperature crystallization (ºC)	886−776	802−755	760−738	747−714	664−663
Pressure crystallization (MPa)	300−250	250−200?	200−100	200−100	200−100
Initial water content (%)	2.5	2.5	2.5	2.5	2.5?
Crystallization water content (%)	6.97	5.04	5.13	5.2	5.33
Water fugacity (MPa)	242	117	112	109	98
Joint families (strike and dip)	N-0°−20°-E (subv.) N-80°−100°-E (subv.)	-	N-20°−40°-E (subv.) N-100º-E (subv.)	-	N-10°−20°-E (subv.) N-50°-E (52ºSE) N-110°-E (subv.)
Spacing family joints (m)	3/7	-	1/0.5	-	3/2.5/3
Quarries	34% quarries in this lithology	15% quarries in this lithology	46% quarries in this lithology	1% quarries in this lithology	4% quarries in this lithology

PCBG: Coarse-grained porphyritic biotite granite; FMIG: Fine-medium-grained inequigranular biotite granite; FBG: fine-grained biotite granite; FGN: fine-grained granite with nodules; TMTG: two mica tourmaline-bearing granite; MMEs: Mafic microgranular enclaves; mineral abbreviations after Warr (2021); L-P: low peraluminous; f-P: felsic peraluminous; -: non considered. Water content and fH_2O were estimated for pressures of 300 MPa (PCBC) and 150 megapascals (rest of granite facies) and temperature obtained from the zircon saturation model (further details in Table 1 S)

medieval water mills located very close by. The facies used exclusively for this purpose is the PCBG. Despite the fact that the predominant facies in the area studied is the FBG and that it is a granite more resistant to erosion than the PCBG, no remains of stone for medieval water mills made in the FBG have been observed. One of the possible reasons for this absence is the reduced spacing of the joint planes of the FBG, which does not allow pieces of these dimensions to be obtained (Figs. 7B and 11A). Somehow the medieval stonemasons knew that the

Fig. 12 (**A**) Aborted extraction of a large millstone on the PCBG. These millstones were used in medieval hydraulic mills in the area. (**B**) Hole left by the extraction of one of these millstones on which some of the participants of the XI Geological Congress of Spain, to be held in Ávila in 2024, were placed. (**C**) Small superficial historical quarry in the FMIG at Point of Interest 5, showing a stepwise front with abundant wedge slots to cut the rock in the N-S direction. Note that the E-W joint is partly filled with a silica precipitate. (**D**) Lintel doorway of the Verdugo Palace (century XVI) built with the FMIG

most favourable blocometry for making these large millstones was the PCBG. According to the current stonemasons of the Cardeñosa locality, the extraction technique of these millstones did not consist in cutting the blocks with wedges and then crushing them until a cylindrical piece was obtained. The technique consisted of selecting a large outcrop free of diaclases. A circle of the required diameter was drawn. A groove of a certain depth was then made on the outside of the circle, probably with a sledgehammer. The hammer or chisel was then hammered into the inside of the circle around its entire circumference until it was cut along its entire length, leaving a rounded depression that can be seen in some outcrops near this site (Fig. 12B).

Point of Interest 5: FMIG Historical Quarry

This location (X: 356230.8, Y: 4510248.3; Lat. 40.730623, Long. −4.702521) is primarily of cultural interest (Fig. 10B), but it also provides a valuable opportunity for visitors to observe the FMIG granite in one of the oldest and best-preserved quarries within this granitic facies (Fig. 12C). The workings, which are superficial and comprise up to five steps, have been excavated from the top downwards. The steps exhibit a profusion of wedge slots, facilitating cutting in both the vertical and horizontal planes. The visitor can observe the size of the extracted block, which is smaller than that of POI 3, but larger than that of the POI 1. Furthermore, the visitor can observe the contrasting level of persistence of the diaclase planes. In the E-W direction, the joint planes extend for tens of meters, while in the N-S direction, they only reach a length of one meter, indicating a significant difference in development between the two systems. This phenomenon enables the extraction of elongated blocks in the E-W direction, which are conducive to the fabrication of monumental columns in Ávila and other long pieces (Fig. 12D). Conversely, this process necessitates the execution of numerous incisions by the stonemason in the N-S direction, while minimal incisions are required in the E-W direction (Fig. 12C).

Point of Interest 6: Huge Wedge Slots in PCBG

This location (X: 356318.3, Y: 4510001.0; Lat. 40.728411, Long. −4.701429) is primarily of archaeological interest. The visitor will observe a typical large PCBG boulder with incisions measuring approximately 33 cm (Fig. 9A). These incisions are arranged in a more or less N-S line, similar to the direction of the mineral fabric, marking the so-called grain plane. The incisions, hypothesized to be wedge slots, were designed to split the boulder into a zoomorphic shape due to its rounded aspect. The proximity to the Vettonian castro of Las Cogotas, where abundant vestiges of a significant lithic industry have been found, including numerous verracos and hand mills (Rodríguez-Hernández 2012), suggests that these incisions were made by the "Vettons" to obtain a verraco. To the best of our knowledge, wedge slots of this size are not reported from Iberia, with the exception of reviews of similar wedge slots in ancient Egyptian quarries (García de los Ríos Cobo 2018), where it is hypothesised that they were utilized to house wooden wedges. When moistened with water, these wedges would increase in volume, thereby fracturing the rock by traction. The direction of the mineral fabric in which the incisions are oriented suggests that the "Vettons" were cognisant of the fact that rock would fracture more readily in this direction.

Point of Interest 7: Miarolitic Cavities

This is a notable instance of geological interest (X: 356327.5, Y: 4509968.5; Lat. 40.72812, Long. −4.701313) (Fig. 10C), wherein an outcrop is observed, exhibiting centimeter-sized circular structures. These structures are of a rare occurrence in nature and are known as miarolitic cavities. The interior of these structures is characterized by a high degree of mineral nucleation of tourmaline (blackish in color), while the exterior is predominantly composed of alkali feldspar (whitish rim) (Fig. 13A). These structures, which manifest as bubbles within the melt, are indicative of fluid saturation and a concomitant volatile separation of the melt. The latter phenomenon may be triggered by a water-rich melt that is emplaced in shallow conditions (first boiling), where a significant amount of anhydrous minerals crystallize, thereby enriching the residual melt in water and other fluxing elements (second boiling). The aforementioned criteria are all met by FGN, as it is categorized as one of the granites with the highest water content (5.2%) and is emplaced in shallow conditions (approximately 150 MPa) and with a low proportion of anhydrous minerals (5% by volume) (Table 1).

Conversely, if the cooling had occurred at greater depth, the fluid phase would not have separated, resulting in the retention of boron, water, and other elements in solution. Consequently, the formation of these structures would not have occurred. The outcrop further facilitates the clear visualization of cordierite-rich centimetric nodules, which are characteristic of the FGN (Fig. 13A).

Point of Interest 8: Stoping

This point of interest (X: 356299.6, Y: 4509813.9; Lat. 40.726723, Long. −4.701607) is of a primarily geological nature (Fig. 10C), with visitors able to observe a geological aspect that is prevalent in this area but not commonly observed in nature. Additionally, visitors can observe the sequentiality in the emplacement of two distinct granite facies. The outcrop displays an angular block of PCBG surrounded by fine-grained granite, probably FBG (Fig. 13B). The most straightforward explanation for this association is that the PCBG was emplaced prior to the FBG. Upon arriving at its emplacement site, the FBG encounters a PCBG that has already undergone a significant degree of cooling, resulting in its formation as the wall rock, in this case, the roof of the FBG. The cold wall rock may fracture and detach from the roof in the form of angular blocks, partially sinking into the later granite (FBG). The sunken blocks do not become assimilated or disrupted by the later magma, likely due to a lack of sufficient energy in the latter to cause melting. This process of emplacement is referred to as magma stoping or piecemeal magma stoping. It is noteworthy that the FBG, a passive magma, is capable of invading fractured and foundered PCBG roof blocks; however, it is incapable of continuing its ascent through the crust. This is likely attributable to a process of fluid exsolution, which triggered a rapid crystallization, thereby favoring the melt's capacity for nucleation and leading to the formation of a fine-grained rock, such as FBG.

Point of Interest 9: Network in the PCBG

Geologically, this area is notable for the presence of multiple aplite and pegmatite injections within the apical zone of the PCBG, forming a network zone (X: 356404.9, Y: 4509821.7; Lat. 40.726812, Long. −4.700363) (Fig. 13C). Within this zone, a network of fractures is present in the PCBG, which would inevitably be quite cold if aplites and pegmatites dykes exhibited straight margins. These intrusive bodies may represent melts or fluids generated during the late magmatic or magmatic-hydrothermal transition events of the PCBG itself or another underlying granite, such as the TMTG observed in the vicinity (Fig. 3A). In the first option, fracturing can be attributed to tectonic processes, pressure relaxation, or the exsolved fluid phase itself of PCBG. It is noteworthy that PCBG exhibits the highest water fugacity (see Table 1), suggesting its remarkable capacity for water escape from the magma. This phenomenon can generate

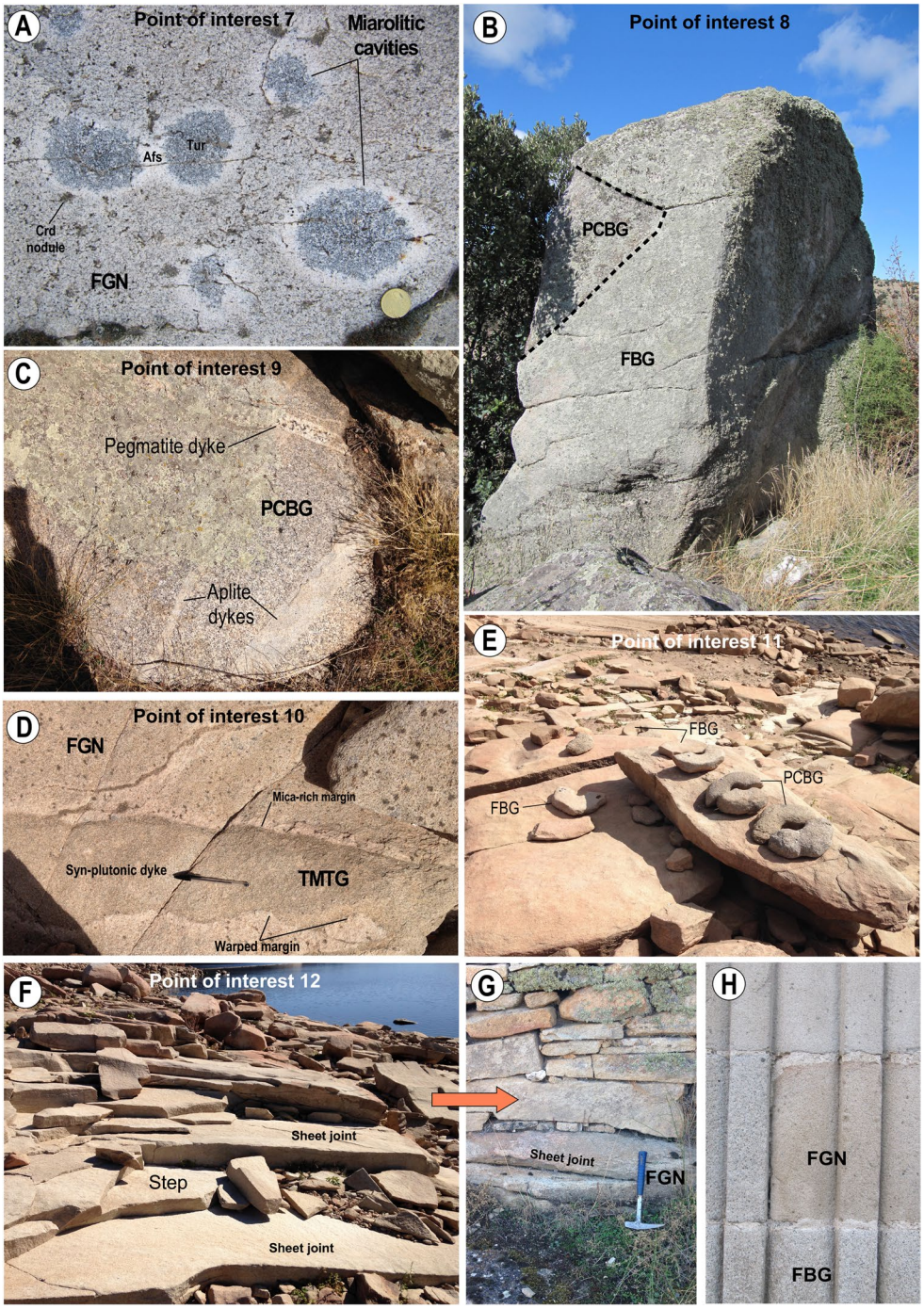

Fig. 13 (**A**) Miarolitic cavities in the FGN close to the Las Cogotas hillfort. Mineral abbreviations after Warr (2021). Miarolitic cavities are defined as bubbles of volatiles that have been separated from a volatile-rich melt in a low-pressure environment. (**B**) Stoping showing an angular PCBG block embedded in a later and colder granite (FBG). (**C**) Network zone in the PCBG with abundant dykes of aplites and pegmatites corresponding to late magmatic or magmatic-hydrothermal transition events. (**D**) Syn-plutonic dyke of TMTG intruding the FGN with warped margins and mica-rich margins (i.e., with hydrated minerals), the latter possibly caused by fluid phase separation and or thermal diffusivity. (**E**) Sample of ancient pre-Roman hand mills found in the surroundings of Castro de Las Cogotas. The mills, all broken, were made of FBG and PCBG, the former being better preserved. (**F**) Small historic surface quarries of FGN at Point of Interest 12, near the Las Cogotas hillfort, probably used by the Vettons for the construction of the Las Cogotas hillfort wall. The quarrymen took advantage of the reduced spacing of the FGN to easily extract blocks, presumably using crowbars. (**G**) Wall of the Las Cogotas hillfort built with FGN and FBG. The photo also shows an outcrop with narrow sheet joints in the FGN. (**H**) Detail of a pilaster of the Cathedral of Ávila, where FGN has been used interchangeably with FBG due to their undeniable similarity, suggesting that both facies were present in the historic quarry from which they were extracted

overpressure within the fractures and pores of the host rock, leading to its fracturing and the precipitation of components carried by the exsolved fluid phase. Conversely, if fluids or near-solidus melts are considered to be linked to TMTG—that is to say, a granite that has been emplaced at a low pressure where the separation of the fluid phase is evident, as indicated by the presence of miarolitic cavities—then the fracturing of PCBG would be a consequence of the pressure of volatiles of TMTG. Aplites and pegmatites would also originate from TMTG.

Point of Interest 10: Syn-plutonic Dyke

This location (X: 356196.9, Y: 4509680.8; Lat. 40.725507, Long. −4.702792) is of geological interest (Fig. 10C) and is noteworthy for illustrating a process of emplacement involving two magmas of approximately coeval origin—a phenomenon that is relatively uncommon in natural settings. The outcrop exhibits a syn-plutonic dike of a two-mica granite (presumably TMTG) that intruded prior to the enclosing

granite (FGN) being fully consolidated (Fig. 13D). The contrast in temperature and viscosity between the two magma types is not sufficient to cause processes of breakage of the cooler granite, as occurs in the piecemeal stoping. However, the two granites interact, and may become mixed and form processes of imperfect mixing (mingling) with lobate margins at the contact between the two granitic types, as occurs in this case. Also, it is noteworthy the abundance of mica in the margins of the dyke, together with the depletion of mica in the adjacent FGN (Fig. 13D). This phenomenon can be explained by a combination of processes, but in our opinion, the more likely is chemical diffusion. In this process, when a hot dyke intrudes into a cooler FGN, a chemical gradient is established between the two systems. Elements involved in mica formation, such as K, Al, F, and H_2O, can diffuse from the host magma into the dyke if chemical equilibrium favors it (e.g., Zhang and Gang 2022). Consequently, a mica-rich margin is formed within the dike, while a mica depletion occurs within the host wall rock (FGN) due to the migration of these elements into the dike. This process is particularly effective at high temperatures over a sustained period.

Point of Interest 11: Hand Mills

At this site of archaeological interest (X: 356246.6, Y: 4509680.8; Lat. 40.725508, Long. −4.702204) (Fig. 10D), visitors can observe a selection of millstones crafted by the ancient inhabitants of the Las Cogotas hillfort. These artefacts offer valuable insight into the technological practices and daily life of the region's prehistoric communities. The mills in question are hand mills of similar size, crafted from the two predominant lithologies of the area: the FBG and the PCBG (Fig. 13E). It is noteworthy that all of the mills are in a state of disrepair, with those belonging to the FBG exhibiting superior preservation. This phenomenon can be attributed to the higher proportion of minerals within the FBG that possess a greater resistance to alteration and abrasion, such as quartz (see Petrographic characterization section).

Point of Interest 12: FGN Historical Quarry

At this point of cultural heritage (X: 356326.5, Y: 4509691.3; Lat. 40.725624°, Long. −4.701261°) (Fig. 10B), visitors can view a historical quarry where one of the granite types used in the monuments of the city of Ávila was extracted. This granite is of the type FGN. The petrological characteristics of the granite are delineated in Table 1. In the area of interest, there is evidence of an ancient surface work (likely executed by the Vettons) in the proximity of the Vetton Cogotas hillfort (see Fig. 13F). Of note is the close spacing of sheet joints, a feature that likely facilitated the efficient extraction of the stone. The use of crowbars in the extraction of slabs for the construction of the Las Cogotas hillfort is a probable hypothesis. The construction of these walls was executed without the use of foundations, directly on the rock itself, employing a technique known as dry masonry (Fig. 13G). This site exemplifies the utilization of a characteristic, namely the intense subhorizontal splitting of fine-grained granites FGN and also FBG, by the Vettons for construction purposes. In the monuments of Ávila, this granite is frequently observed in conjunction with the FBG, as evidenced by its presence in the pilasters of the Cathedral of Ávila (Fig. 13H). This association can be attributed to their visually similar appearance. It is plausible that the historic quarry where this granite was extracted contained both granitic facies (FGN and FBG).

Point of Interest 13: Archaeological Classroom

This location (X: 352817.4, Y: 4511568.8; Lat. 40.74191, Long. −4.743236) is primarily of archaeological interest (Fig. 10A). The main attraction of this POI is the Municipal Museum of Cardeñosa (Fig. 14A). This institution houses a collection of original artifacts and replicas of the Vetton culture, offering insights into the daily life of the Vettons and highlighting the importance of granite in their culture. The exhibition includes information about the history of the excavations at Las Cogotas hillfort, as well as miniature recreations of the site (Figs. 14B, C and D). These miniature reconstructions allow visitors to distinguish different features of the site, such as the Vetton settlement, the necropolis, the different walls with their entrances, the fields of driven stones and the dwellings inside the walls. This municipal museum is the starting point of the archaeological routes organized in the area related to the Vetton hillfort of Cogotas.

Concluding Remarks

Our multifaceted approach, which involved geological cartography, an inventory of quarries, allowed us to confirm the extraction of up to five different types of granite in the Cardeñosa-Cogotas area. These granites were used in monuments in Ávila and in the expansion area north of Cardeñosa. The abundance of ancient quarries in the area confirms that it was probably the most important center of granite extraction in the World Heritage Site of Ávila, Spain. The amount of each type of granite available in the area, the strike, dip and spacing of joints, as well as the presence or absence of planar fabrics in the granite, greatly influenced the extraction, supply, and use of certain types of granite in the historical monuments of the city of Ávila. Two main types of granite were extracted and used in the monuments:

Fig. 14 Archaelogical Classroom of Las Cogotas Hillfort. (**A**) Entrance to the Town Hall of Cardeñosa, where the archaeological classroom is located. (**B**) Miniatures of zoomorphic sculptures in granite (PCBG), called verracos. The large spacing of the joints in this granite favored the use of this granite almost exclusively for the elaboration of these sculptures. (**C**) Recreation of the hillfort wall and the Vetton house wall. (**D**) Model of the Vetton Hillfort of Las Cogotas

the PCBG and the FBG. On the other hand, the scarcity of the FGN and the unfavorable arrangement of the joints in the TMTG penalized its use. The utilization of diverse granitic facies in the monuments indicates either that a specific granite type exhibited optimal suitability for a specific area of the monument or that there was concurrent exploitation of multiple granitic facies. The utilization of granite from the pre-Roman period to the present era in the specified area enables the establishment of two key observations. Firstly, the progressive reduction in the dimensions of the wedges

prior to the advent of mechanization can be ascertained. Secondly, historical quarries were characterized by diminutive dimensions and superficial depth. However, these characteristics underwent an augmentation as the employment of augers, explosives, and diamond wire for cutting was introduced over the course of time. Moreover, the results of our detailed geological study demonstrate that the emplacement of the granites occurred sequentially and, in some cases, concurrently, under conditions of low pressure (300 − 100 MPa). The findings indicate that in this part of the Iberian Massif, the granites are emplaced under relatively shallow conditions, developing contact metamorphism and miarolitic cavities, both in FGN and TMTG. The utilization of the F-An-Or pseudoternary plot, in conjunction with the observed similarities in REE patterns, lends support to the hypothesis that all post D3 granites of the Cardeñosa-Cogotas area could be cogenetic in origin. Furthermore, the disparities in the major elements composition of the most frequently utilized granite facies in monuments from Ávila, in comparison to the quarry samples are attributable to the mobilization of the mortars present in the monuments. Regarding the tourism route, the wealth of multidisciplinary information available has allowed the creation of mixed tourist itineraries highlighting points of interest with a broad geological focus, sites of cultural heritage such as historical quarries, and sites of archaeological interest. Conversely, the amalgamation of these subjects with the extant archaeological classrooms related to the Cogotas hillfort in the area ensures the success of the proposed route in this study. Compared to other national and international geotourism routes that combine geological and cultural elements with museum visits, the itinerary presented here offers distinctive features. Within a short distance, visitors can trace the evolution of stone-cutting techniques from pre-Roman times to the modern era and see how geological factors influence quarry design, extraction methods, and the production of ashlar blocks and millstones before mechanization. The itinerary also highlights geological and petrogenetic aspects of the quarried granites—knowledge largely unpublished and rarely accessible in other geotourism initiatives. For example, the pressure, temperature, and water content estimates for each magma emplacement site help visitors understand the mesostructures observed along the route. This itinerary enhances visitors' understanding of geological processes by bridging the gap between scientific knowledge and public awareness of the natural environment. Finally, the implementation of this route will guarantee the preservation of a substantial geological, cultural, and archaeological heritage.

Supplementary Information The online version contains supplementary material available at https://doi.org/10.1007/s12371-025-01226-x.

Acknowledgements The first author is in doubt with Chari Sansegundo, who kindly provided beautiful photos of the Archaeological Classroom of Las Cogotas Hillfort, and people from the Town Council of Cardeñosa for providing information on the tools used by Cardeñosa stonemasons and for demonstrations performed on granite cutting in the zone. We are grateful to the two anonymous reviewers for their constructive feedback, which significantly contributed to clarifying our ideas and enhancing the quality of the manuscript. The first author dedicates this work to his recently deceased father, Teodoro López (Fig. 11 C), who often accompanied him to the Cardeñosa quarries.

Author Contribution **F.J. López-Moro**: Writing – original draft, Validation, Supervision, Investigation, Funding acquisition, Formal analysis, Data curation, Conceptualization. **M. López-Plaza**: Writing – review & editing, Validation, Supervision, Methodology, Investigation, Formal analysis, Data curation, Conceptualization. **M. González-Sánchez**: Writing – review & editing, Validation, Investigation. **J.I. García de los Ríos Cobo**: Writing – review & editing, Validation, Supervision, Project administration, Methodology, Investigation, Formal analysis, Data curation, Conceptualization. **A. Herrero Hernández**: Writing – review & editing, Validation, Supervision.

Funding Open Access funding provided thanks to the CRUE-CSIC agreement with Springer Nature. This work has benefited from the following research grants: (i) research grant from the Institución Gran Duque de Alba to the first author; (ii) project PGC2018-098151-B-I00, funded by the National Research Agency and the European Union; and (iii) project 18KAG8/463AC01, funded by the University of Salamanca.

Declarations

Ethical Conduct This article contains no studies with human or animal subjects.

Conflict of interest The author declares no competing interests.

References

American Geological Institute (1957) Glossary of Geology and Related Sciences. American Geological Institute, Washington DC

Arnold A, Zehnder K (1989) Salt weathering on monuments. In: Zezza F (ed) Proc. 1st Int. Symposium on the Conservation of Monuments in the Mediterranean Basin, Bari, pp 31–58

Asociación Española de Normalización (2020) Métodos de ensayo para piedra natural. Estudio petrográfico (UNE-EN 12407)

Ayuntamiento de Ávila (2025) Ávila Muralla. La Primera Muralla. https://muralladeavila.com/es/historia/la-primera-muralla. Accessed 3 June 2025

Azofra Agustín E, López-Plaza M (2020) Cambios derivados por el uso del granito de las canteras históricas de Cardeñosa y Mingorría (Ávila) en el paisaje monumental del Centro-Sur de Castilla y León desde el medievo hasta el siglo XVIII. Nodos. Artes y Humanidades Arte y Patrimonio Cultural. Sección C. https://bit.ly/3vroTx9. Accessed 2 Apr 2025

Ballouard C, Poujol M, Boulvais P, Branquet Y, Tartèse R, Vigneresse JL (2016) Nb-Ta fractionation in peraluminous granites: a marker of the magmatic-hydrothermal transition. Geology 44:231–234

Bellido F, Capote R, Casquet C, Fuster JM, Navidad M, Peinado M, Villaseca C (1981) Caracteres generales Del cinturón hercínico En El sector Oriental Del sistema central Español. Cuad Geológicos Ibéricos 7:15–51

Castro A (2013) Tonalite-granodiorite suites as cotectic systems: a review of experimental studies with implications to granitoid petrogenesis. Earth Sci Rev 124:68–95

Cox KG, Belt JD, Pankhurst RJ (1979) The interpretation of igneous rocks. George, Allen and Unwin, London. https://doi.org/10.1007/978-94-017-3373-1

Debon F, Le Fort P (1983) A chemical mineralogical classification of common plutonic rocks and association. Earth Sci 73:135–149

Dowling RK (2010) Geotourism's global growth. In: Newsome D, Dowling RK (eds) Geotourism: the tourism of geology and landscape. Goodfellow, Oxford, pp 1–17

Ebadi A, Johannes W (1991) Beginning of melting and composition of first melts in the system Qz-Ab-Or-H<Subscript>2</Subscript>O-CO<Subscript>2</Subscript>. Contrib Mineral Petrol 106:286–295

Frost BR, Barnes CG, Collins WJ, Arculus RJ, Ellis DJ, Frost CD (2001) A geochemical classification for granitic rocks. J Petrol 42:2033–2048

García de los Ríos Cobo JI (2018) La Cantería Tradicional. El Laboreo de La Piedra. De la Montaña al Monumento. SIEMCALSA, Valladolid

García-Talegón J (1996) Paleoalteraciones y alteraciones actuales de rocas silíceas: implicaciones en el paisaje y su comportamiento como materiales de construcción. Dissertation, University of Salamanca

Hobbs BE, Means WD, Williams PF (1976) An outline of structural geology. Wiley, Australia

Holloway JR, Blank JG (1994) Application of experimental results to C-O-H species in natural melts. Rev Mineral Geochem 30:187–230

Hose TA (1995) Selling the story of britain's stone. Environ Interpret 10:16–17

Hose TA (2000) European geotourism—geological interpretation and geoconservation promotion for tourists. In: Barettino D, Wimbledon WAP, Gallego E (eds) Geological heritage: its conservation and management, Instituto Tecnológico GeoMinero de España, pp. 127–146

IGME (1982) Mapa Geológico de España. Escala 1:50.000. Cardeñosa (506). Instituto Geológico y Minero de España, Madrid

Irber W (1999) The lanthanide tetrad effect and its correlation with K/Rb, Eu/Eu∗, Sr/Eu, Y/Ho, and Zr/Hf of evolving peraluminous granite suites. Geochim Cosmochim Acta 63:489–508

Jung S, Pfänder JA (2007) Source composition and melting temperatures of orogenic granitoids: constraints from CaO/Na<Subscript>2</Subscript>O, Al<Subscript>2</Subscript>O<Subscript>3</Subscript>/TiO<Subscript>2</Subscript>and accessory mineral saturation thermometry. Eur J Mineral 19:859–870

Kuno H (1960) High-alumina basalts. J Petrol 1:121–145

Larsen ES (1938) Some new variation diagrams for groups of igneous rocks. J Geol 46:505–520

López Fernández MI (2002) Guía de La arquitectura civil Del Siglo XVI En Ávila. Cuadernos de La escuela oficial de turismo de Castilla y León. Fundación Cultural de Santa Teresa, Ávila

López-Moro FJ, López-Plaza M, García de los Ríos Cobo JI (2021) La Tierra de Las Mil canteras: caracterización geológica Del área granítica de Cardeñosa-Mingorría y Alrededores de Ávila. Azofra Agustín E and Gutiérrez-Hernández AM (coord) El Uso de Los materiales pétreos En El patrimonio monumental. Alamar Libros, Salamanca, pp 15–18

López-Moro FJ, Díez Montes A, Llorens González T, Sánchez García T, Timón-Sánchez SM (2023) Metales Críticos: a tool for processing geochemical and chemical mineralogical data and obtaining geothermobarometric constraints in granites and rare-metal granites. Macla 27:75–76

López-Moro FJ, Díez-Montes A, Timón-Sánchez SM, Llorens-González T, Sánchez-García T (2024) Peraluminous rare metal granites in iberia: geochemical, mineralogical, geothermobarometric, and petrogenetic constraints. Minerals 14:249. https://doi.org/10.3390/min14030249

López-Plaza M (2024) Claves e Hitos sobre El Uso diversificado de La Piedra En El exterior de Los Monumentos de Ávila. In: Olivero Guidobro S (ed) (coord) Materiales, técnicas, estrategias y resultados. Planteamientos Humanos ante Los retos socio-culturales. Dykinson, S.L., Madrid, pp 554–581

Luth WC, Jahns RH, Tuttle OF (1964) The granite system at pressures of 4 to 10 Kilobars. J Geophys Res 69:759–773

Moore G, Vennemann T, Carmichael ISE (1998) An empirical model for the solubility of H_2O in magmas to 3 kilobars. Am Mineral 83:36–42

Moreno Blanco R, Azofra Agustín E, López Plaza M (2022) Ávila monumental. Ocho Siglos alzándose En Granito. In: Azofra Agustín E, García-Talegón J, Gutiérrez-Hernández AM (eds) La Piedra En El patrimonio monumental. Ediciones Universidad de Salamanca, Salamanca, pp 137–168

Pichavant M (1981) An experimental study of the effect of Boron on a water saturated haplogranite at 1 Kbar vapour pressure. Contrib Mineral Petrol 76:430–439

Pichavant M, Erdmann S, Kontak DJ, Michaud JAS, Villaros A (2024) Trace element partitioning in strongly peraluminous rare-metal silicic magmas—implications for fractionation processes and for the origin of the macusani volcanics (SE Peru). Geochim Cosmochim Acta 365:229–252

Reynard E (2008) Scientific research and tourist promotion of geomorphological heritage. Geogr Fis Din Quat 31:225–230

Rodríguez-Hernández J (2012) Los procesos técnicos de La cantería Durante La Segunda edad Del Hierro En El occidente de La meseta. Zephyrus 70:113–130

Sun SS, McDonough WF (1989) Chemical and isotopic systematics of oceanic basalts: implications for mantle composition and processes. In: Saunders AD, Norry MJ (eds) Magmatism in ocean basins. Geological Society Special Publication, Geological Society, London, pp 313–345

Talavera C, Montero P, Bea F, Lodeiro FG, Whitehouse M (2013) U-Pb zircon geochronology of the Cambro-Ordovician metagranites and metavolcanic rocks of central and NW Iberia. Int J Earth Sci 102:1–23

Taylor SR, McLennan SM (1985) The continental crust: Its composition and evolution. Blackwell, Oxford

Tuttle OF, Bowen NL (1958) Origin of Granite in the Light of Experimental Studies in the System NaAlSi3O8–KAlSi3O8–SiO2–H2O. The Geological Society of America, New York

Vera JA, Ancochea E, Barnolas A, Bea F, Calvo JP, Civis J, De Vicente G, Fernández-Guianotti J, García Cortes A, Pérez-Estaún A, Pujalde V, Rodríguez-Fernández LR, Sopeña A, Tejero R (2004) Introducción. In: Vera JA (ed) Geología de España, 1st edn. Sociedad Geológica de España and Instituto Geológico y Minero de España, Madrid, pp 3–17

Villaseca C, Barbero L, Herreros V (1998) A re-examination of the typology of peraluminous granite types in intracontinental orogenic belts. Trans R Soc Edinb Earth Environ Sci 89:113–119

Warr LN (2021) IMA-CNMNC approved mineral symbols. Mineral Mag 85:291–320. https://doi.org/10.1180/mgm.2021.43

Watson EB, Harrison TM (1983) Zircon saturation revisited: temperature and compositional effects in a variety of crustal magma types. Earth Planet Sci Lett 64:295–304

Zhang Y, Gang T (2022) Diffusion in melts and magmas. Rev Mineral Geochem 87:283–337